Bioactive Materials 6 (2021) 794–809

Contents lists available at ScienceDirect

Bioactive Materials

journal homepage: http://www.keaipublishing.com/biomat

Cyanine conjugates in cancer theranostics

Yang Li[a], Yiming Zhou[a], Xiuli Yue[b,**], Zhifei Dai[a,*]

[a] Department of Biomedical Engineering, College of Engineering, Peking University, Beijing 100871, China
[b] School of Environment, Harbin Institute of Technology, Harbin 150001, China

ARTICLE INFO

Keywords:
Cyanine conjugate
Cancer theranostics
Therapeutic agent
Nanocarrier
Clinical translation

ABSTRACT

Cyanine is a meritorious fluorogenic core for the construction of fluorescent probes and its phototherapeutic potential has been enthusiastically explored as well. Alternatively, the covalent conjugation of cyanine with other potent therapeutic agents not only boosts its therapeutic efficacy but also broadens its therapeutic modality. Herein, we summarize miscellaneous cyanine–therapeutic agent conjugates in cancer theranostics from literature published between 2014 and 2020. The application scenarios of such theranostic cyanine conjugates covered common cancer therapeutic modalities, including chemotherapy, phototherapy and targeted therapy. Besides, cyanine conjugates that serve as nanocarriers for drug delivery are introduced as well. In an additional section, we analyze the potential of these conjugates for clinical translation. Overall, this review is aimed to stimulate research interest in exploring unattempted therapeutic agents and novel conjugation strategies and hopefully, accelerate clinical translation in this field.

1. Introduction

Cancer is a major public health problem and has become a leading cause of mortality worldwide. Unfortunately, tumor heterogeneity, metastasis and therapy resistance collectively make cancer a formidable disease and ultimately lead to therapeutic failures. The combination of diagnostic imaging and therapeutic intervention is a newly emerging modality developed to address these challenges, known as cancer theranostics. With its concept first introduced by John Funkhouser in 1998, theranostic agent features a single integrated system with simultaneous therapeutic and diagnostic competencies [1]. Generally, it is comprised of therapeutic agent and contrast agent that give rise to therapeutic output and diagnostic readout, respectively; sometimes a targeting warhead is also integrated to enhance its tumor targeting effect. Beyond the basic therapeutic effect, it is the capability to extract real-time diagnostic information from complex biological systems that makes theranostic agent a promising platform, which can be broadly divided into two aspects: disease-related information comprising the expression profile of drug target and localization of primary or even metastasized tumor sites; therapeutic process–associated information including pharmacokinetics, drug activation and therapeutic efficacy [2].

Cyanine is a subcategory of polymethine dye family, the structure of which is characterized by two nitrogen centers linked by a π-conjugated polymethine chain [3]; generally, its two nitrogen atoms are independently embedded in heterocycles such as pyrrole, pyridine, indole, thiazole, benzothiazole, etc. (Fig. 1) [4]. As one of the most investigated fluorogenic cores for the construction of fluorescent probes, cyanine possesses meritorious attributes: first, favorable fluorescence properties including high molar absorptivity, narrow absorption/emission band and tunable spectroscopic profile across the UV/Vis and near-infrared (NIR) range [5–7]; second, excellent biocompatibility and low toxicity [8]. While other fluorescent dyes possess either relatively low molar absorptivity (e.g. coumarin, diketopyrrolopyrrole) or limited emission maximum (e.g. rhodamine, fluorescein) [9]. Moreover, cyanine itself has been explored as a phototherapeutic agent owing to its photoconversion ability, especially those emitting fluorescence in NIR window with deep tissue penetration—indocyanine green (ICG), for instance Ref. [10]. As a photosensitizer, however, cyanine suffers from low photoconversion efficiency and poor photostability, which consequently leads to inadequate phototherapeutic efficacy. By contrast, conjugation with other potent therapeutic agents not only boosts its therapeutic efficacy but also broadens its therapeutic modality. As these theranostic cyanine conjugates normally function in living systems, cyanine dyes emitting in the NIR range (> 650 nm) are preferred for conjugation, especially for in vivo characterization, due to inherent

Peer review under responsibility of KeAi Communications Co., Ltd.
* Corresponding author.
** Corresponding author.
E-mail addresses: xiulidx@163.com (X. Yue), zhifei.dai@pku.edu.cn (Z. Dai).

https://doi.org/10.1016/j.bioactmat.2020.09.009
Received 7 August 2020; Received in revised form 11 September 2020; Accepted 11 September 2020

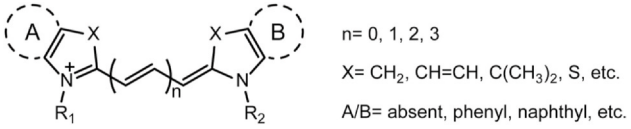

Fig. 1. The typical chemical structure of cyanine dye.

advantages such as deep tissue penetration, less photocytotoxicity, reduced light scattering and minimal autofluorescence [11,12]. Furthermore, several heptamethine cyanine dyes including IR-780, IR-783, IR-808 (MHI-148) have demonstrated preferential accumulation and retention in tumor tissues [13]. This unique property was collaborately mediated by the prevailing activation of membrane-bound organic-anion-transporting polypeptides and increased mitochondrial membrane potential in cancer cells [14]; and the formation of covalent albumin adducts was proposed as well [15]. Consequently, these heptamethine cyanine scaffolds are frequently employed to develop theranostic cyanine conjugates. And the conjugation with other active components (drugs, targeting ligands, etc.) is accomplished via various functional groups on cyanine scaffold (Fig. 2).

Previous reviews aiming to highlight the potential of cyanine in cancer theranostics are quite limited. For instance, Thomas et al. briefly introduced the application of heptamethine cyanine–based nanocomplexes with particular emphasis on phototherapy, while gene therapy and chemotherapy are rarely addressed [16]. Our group has also summarized miscellaneous cyanine-based nanoprobes that are utilized as imaging/phototherapeutic agents, some of which further co-encapsulate potent therapeutic compounds to effectuate synergetic photochemotherapy [17]. The above work mainly focused on the phototherapeutic effect of cyanine dyes which are either encapsulated or assembled in complex nanoconstruct. In this work, however, we pay attention to cyanine-based theranostic agents that exploit the therapeutic capability of other drugs by covalent conjugation. As cyanine dyes almost consistently act as diagnostic tools in cyanine–therapeutic agent conjugates, this review is classified according to the therapeutic modalities, namely, chemotherapy, phototherapy and targeted therapy. Additionally, a subset of cyanine conjugates that function as nanocarriers for the delivery of therapeutic agents are introduced.

2. Chemotherapy

Chemotherapy is one of traditional cancer treatments that utilizes anti-cancer drugs, also called chemotherapeutic agents, as part of a standardized chemotherapy regimen. The anti-tumor effect is derived from the toxicity towards rapidly dividing cells as tumor is typically characterized by uncontrolled proliferation; therefore, tumors featuring a relatively low growth rate are less susceptible to chemotherapeutic agents. Because of its non-selectivity over other fast-dividing cells, chemotherapy can induce many adverse effects encompassing nausea and vomiting, myelosuppression, gastrointestinal toxicity, alopecia, etc. [18]. To circumvent these defects, conjugation with tumor-avid heptamethine cyanine dyes for tumor-targeted drug delivery represents a reasonable approach. Besides, cyanine–chemotherapeutic agent conjugates provide a platform to assess chemotherapy status.

Based on mechanism of action, chemotherapeutic agents are divided into various categories; those reported in the formulation of cyanine conjugates and their representative drugs are listed as below: antimetabolites (e.g., methotrexate, gemcitabine), alkylating agents (e.g., nitrogen mustard, cisplatin, temozolomide), topoisomerase inhibitors (e.g., camptothecin), mitotic inhibitors (e.g., paclitaxel). Generally, the conjugation process takes advantage of the innate reactive group (–OH, $–NH_2$, –COOH) on drug molecules to facilitate the formation of a biocompatible ester or amide linkage. The linker can be designed as cleavable (e.g., disulfide bond) or non-cleavable (e.g., amide bond), each exhibiting distinct mode of action and thus being reviewed separately.

2.1. Conjugates with non-cleavable linker

Direct conjugation between cyanine dye and chemotherapeutic agent, forming a non-cleavable amide/ester bond, is a commonly adopted strategy (Fig. 3A). For instance, gemcitabine has an amino group on the cytosine ring and was demonstrated to conjugate with various cyanine fluorophores through *N*-alkylated hexanoic acid side chain (**1**) [19] or *meso*-substituted 3-mercaptopropionic acid linker (**2**) [20,21]. The 5′-OH should be avoided because it needs to be thrice phosphorylated to generate the pharmacologically active form. These cyanine-gemcitabine conjugates exhibited anti-tumor effect comparable to that of unconjugated drug, and tumor accumulation in intracranial or subcutaneous glioblastoma xenograft model; besides, the pharmacokinetic information was easily acquired via NIR imaging (Fig. 3B). In a similar approach, nitrogen mustard containing a phenolic hydroxyl group was conjugated to IR-808 (**3**) for tumor-targeting delivery [22]. On the other hand, the increased reactivity of phenolic hydroxyl group also allows direct conjugation with *meso*-Cl under intense conditions,

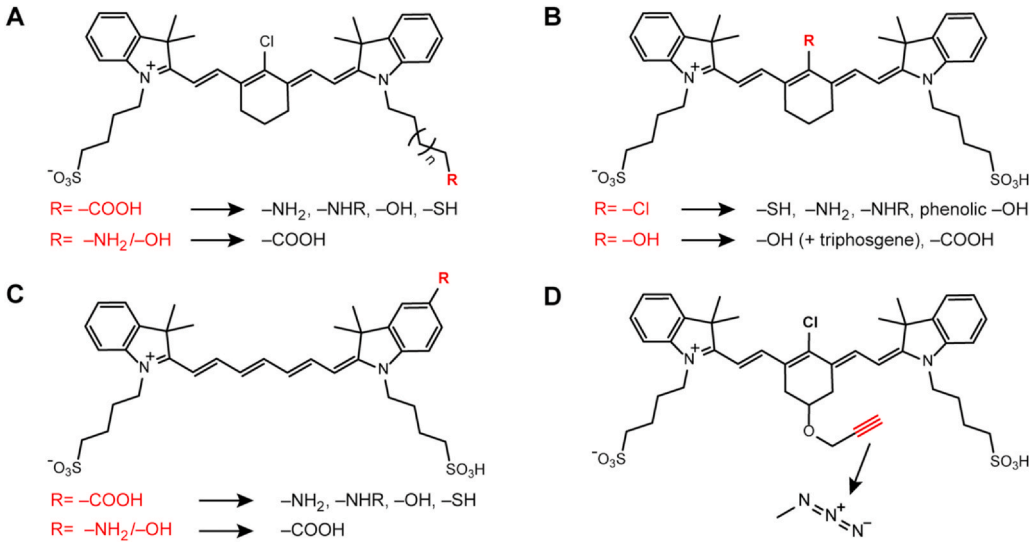

Fig. 2. The conjugation strategy between cyanine and other active components via (A) *N*-alkylated side chain, (B) *meso*-substituent, (C) heterocyclic nucleus, (D) cyclohexene ring.

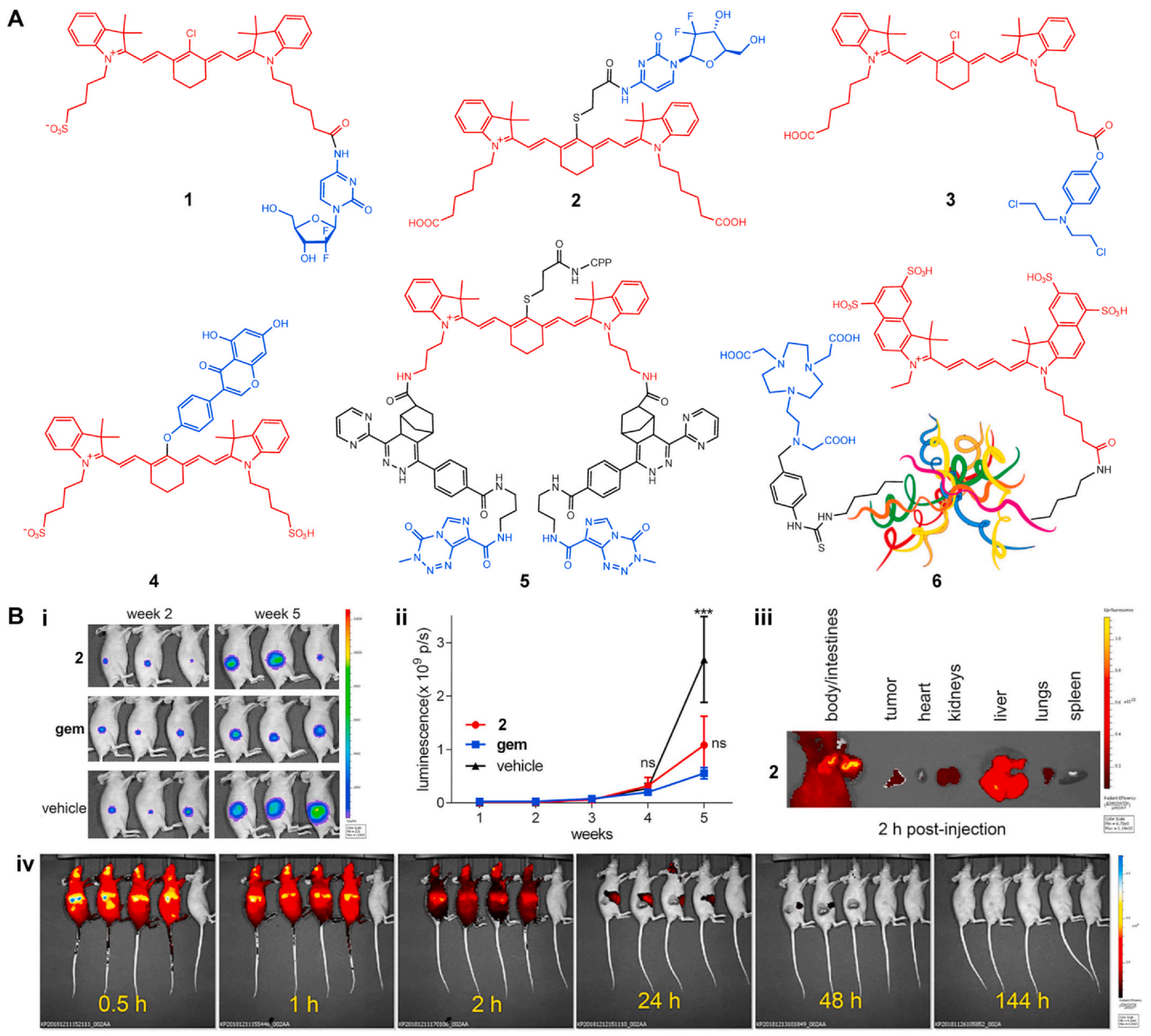

Fig. 3. (A) Cyanine–chemotherapeutic agent conjugates with non-cleavable linker (**1**–**6**). Reprinted with permission from Refs. [25]. (B) In vivo characterization of **2** in mice bearing U87-RFP-Luc subcutaneous tumors. i, luminescence imaging of xenograft model treated with indicated compounds at 2 and 5 weeks after treatment. Ii, corresponding mean tumor luminescence with SEM over 5 weeks (n = 3) and there is a significant difference between 2/gem and the vehicle group at 5 weeks ($p < 0.001$). Iii, fluorescence imaging of main organs and tumor dissected at 2 h p.i. of 2, showing tumor localization. Iv, pharmacokinetic profile of **2** acquired via fluorescence imaging at 0.5, 1, 2, 24, 48, and 144 h p.i. with an uninjected control (last mouse in each view). Reprinted with permission from Ref. [20].

e.g., the formation of genistein-IR783 conjugate (**4**) under NaH/DMF [23].

Unlike conventional amide/ester linkage, the Cy7-cell penetrating peptide conjugate appended with two norbornene moieties was coupled to diaryl-tetrazine modified temozolomide (**5**) via click chemistry [24]. For enhanced targeting, Kang et al. employed tumor-targeting transferrin as warhead and carrier at the same time [25]. A novel cytotoxic chelating agent (*N*-NE3TA) and Cy5.5 were conjugated to transferrin via sulfocarbamide and amide linkage (**6**) for iron chelation anti-tumor therapy and NIR fluorescence (NIRF) imaging, respectively.

2.2. Conjugates with cleavable linker

Prodrugs that are selectively activated at tumor site by internal or external stimuli can decrease off-target toxicity and enhance therapeutic index for chemotherapy. Internal stimuli, such as low pH, hypoxia, ROS, intracellular thiols and overexpressed enzymes, are inhered in tumor cells or tumor microenvironment while external stimuli including photo-irradiation, temperature etc. are applied factitiously [26]. The introduction of prodrug strategy to cyanine-chemotherapeutic agent conjugate via a cleavable linker has turned it into stimuli-responsive theranostic agent which can not only exert controllable chemotherapeutic effect but also simultaneously monitor its biodistribution and activation in a spatiotemporal manner. These theranostics, possessing covalently linked drugs and cyanine dyes, remain inactive in normal tissues but are activated and disintegrated into individual components at tumor site. Generally, cyanine dyes displayed different spectroscopic profile in the conjugated and unconjugated state, which underpins the monitoring mechanism of prodrug activation.

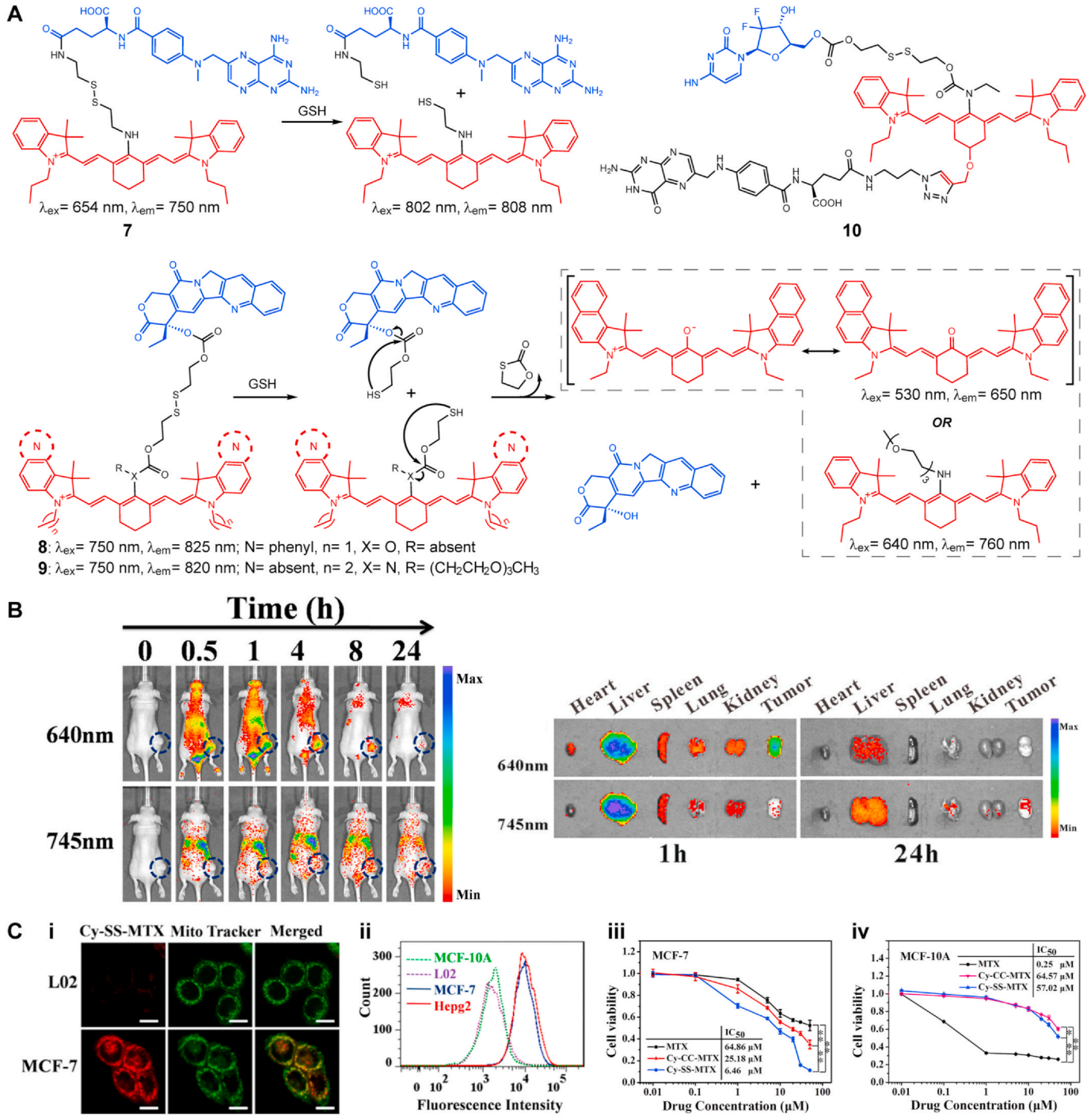

Fig. 4. (A) Cyanine–chemotherapeutic agent conjugates with GSH-cleavable linker (**7**–**10**). (B) In vivo NIRF imaging of MCF-7 xenograft model (left) and ex vivo NIRF imaging of normal organs and tumors (right) at indicated time points after intravenous injection of **7** via biodistribution (640 nm) and activation (745 nm) channel. (C) I, confocal images of L02 normal cells and MCF-7 cancer cells cultured with **7** for 0.5 h, showing cancer-selectivity and preferential localization in mitochondria. Ii, flow cytometry analysis of cellular uptake of **7** in L02 normal cells, MCF-10A breast cancer progression cells, and two cancer cell lines, MCF-7 and Hepg2. Iii-iv, cytotoxicity of MTX, **7**, and Cy–CC–MTX on MCF-7 cells and MCF-10A cells. *, $P < 0.05$; **, $P < 0.01$. Reprinted with permission from Ref. [27].

2.2.1. GSH-cleavable disulfide bond

The elevated GSH levels in various cancers is frequently exploited as an internal stimulus in prodrug design. Accordingly, disulfide bond that can be readily cleaved by GSH is engineered into linker structure as a responsive element (Fig. 4A). For example, the *meso*-Cl of IR780 was conjugated to the γ-COOH of methotrexate via a 2,2′-dithiobis (ethylamine) linker (**7**, Cy–SS–MTX) [27]. Upon GSH-promoted cleavage, the intramolecular charge transfer between cyanine and methotrexate was disrupted; consequently, a new absorption peak at 802 nm arose while the initial peak at 654 nm disappeared and the fluorescence peak at 750 nm also shifted to 808 nm. This allowed monitoring its biodistribution (λ_{ex} = 640 nm channel) and bioactivation (λ_{ex} = 745 nm channel) at the same time (Fig. 4B). Besides, the prodrug exhibited excellent tumor-targeting capability and better anti-tumor efficiency than methotrexate and its non-cleavable counterpart with lower toxicity (Fig. 4C). For drugs with a reactive hydroxyl group (e.g., camptothecin, gemcitabine), organocarbonate linkage can substitute the above amide linkage using a 2,2′-dithiodiethanol linker; moreover, it is

susceptible to the nucleophilic –SH generated after activation and thus can be further cleaved from the drug molecule via an intramolecular cyclization process. As is the case for conjugate **8**, the disulfide bond cleavage and subsequent self-immolation of the resultant half-linker led to the release of camptothecin in its original structure and tautomerization of cyanine fluorophore with a drastic fluorescence shift from 825 nm to 650 nm [28]. Zhang and colleagues reported a similar cyanine-camptothecin conjugate featured an analogous carbamate linkage on the cyanine side [29]. **9** underwent similar activation process and also displayed a significant hypsochromic shift in the emission maximum (from 820 nm to 760 nm). The sole difference was that the enol-ketone tautomerization was prohibited and changes in spectrum signature were ascribed to altered electron-density distribution along the polymethine chain. This unique carbonate-carbamate linkage design was employed in a Cy7-gemcitabine conjugate (**10**) as well and a folate moiety was incorporated at the cyclohexene ring for enhanced tumor-targeting delivery [30].

2.2.2. Biodegradable ester bond

Another common prodrug strategy takes advantage of a biodegradable ester linkage that can be cleaved by esterase or environment-mediated hydrolysis. Chlorambucil bearing a reactive carboxylic functionality was shown to form biodegradable ester bond with various cyanine fluorophores. For instance, a phenol-embedded cyanine dye was conjugated to chlorambucil via a phenolic ester linkage and conjugate **11** was readily cleaved in phosphate buffer (Fig. 5A) [31]. Upon ester cleavage, cyanine underwent phenol-quinone tautomerization and π-conjugation pattern of the polymethine chain was restored, accompanied by a pronounced fluorescence enhancement at 720 nm. The release of camptothecin in conjugate **12** relied on a similar tautomerization process initiated by H_2O_2-triggered cleavage of the phenolic ether (Fig. 5B) [32]. And this mode of action may motivate the modular design of substrate-triggered prodrug activation. Rozovsky et al. contrived a series of bifunctional pentamethine cyanine scaffolds with different combinations of –OH, $–NH_2$, –COOH for conjugation with drug and carrier (Fig. 5C) [33]. As a proof-of-concept, they synthesized four cyanine-chlorambucil conjugates and characterized their cleavage profiles in PBS pH 7.4 and cell medium pH 7.4; they found that ester bond could be readily cleaved in both conditions. Conjugates **13a–b** displayed a noticeable enhancement in fluorescence quantum yield but changes in absorption/emission peak were minimal. To implement such conception, they conjugated chlorambucil and somatostatin receptor (SSTR)–specific octreotide amide sequentially to a cyanine scaffold, though at different sites [34]. The conjugated cyanine fluorophore was in NIR emitting enol-form (λ_{em} = 795 nm); after ester biodegradation, it was converted to red emitting ketone-form (λ_{em} = 643 nm). Compared to free chlorambucil, conjugate **14** exhibited greater cytotoxicity in human pancreatic cancer cell line over-expressing SSTR-2 and SSTR-5. In another approach, Luan's group coupled hydrophilic IR820 with the hydrophobic drug paclitaxel (PTX) through a 6-aminocaproic acid linker; the resultant amphiphilic conjugate **15** could self-assemble into nanoparticles in aqueous solution [35]. After EPR-mediated accumulation at tumor site and cellular internalization, the conjugate was able to disassembe due to the degradation of ester linkage catalyzed by low pH and esterase in lysosomes (Fig. 5D). The controllable release of paclitaxel together with the PTT effect of IR820 enabled synergistic chemo-photothermal therapy and improved the anti-tumor efficacy of IR820 or PTX.

2.2.3. NIR light–uncaging strategy

The photo-uncaging strategy, in which drug is released from cyanine conjugate upon photo-irradiation, facilitates the spatiotemporal control over prodrug activation. Especially, NIR light is preferable by virtue of its deep tissue penetration and minimal photocytotoxicity (Fig. 6A). Zhu's lab reported a caged camptothecin prodrug (**16**) based on a photocleavable cyanine backbone [36]. As designed, photooxidative cleavage of the polymethine chain induced self-immolation of the caging tether and ultimately released the drug. The prodrug biodistribution could be tracked in 820 nm emission channel; upon 680 nm light irradiation, a new 535 nm channel emitted from the fragmented Cy-Biotin arised (Fig. 6B). Under photo-irradiation, the activated prodrug exhibited superior antitumor activity than the intact conjugate in MTT assay but was less potent than its parent drug. For more direct photocleavage, Mitra et al. developed a platinum (II) prodrug by conjugating cisplatin with IR797 via a photodetachable O^O bidentate linkage (**17**) [37]. Upon NIR-triggered photoscission of Pt–O bond, an aquated (bioactive) form of cisplatin was released from the conjugate. Concurrently, the singlet oxygen quantum yield was significantly enhanced owing to the incorporation of heavy atom (Pt) and so was the PDT efficacy (Fig. 6C). Besides, the subsequent decomposition process of IR797-acac leads to a decrease in absorbance at 790 nm (Fig. 6D). Under NIR light exposure, the IR797-Platin conjugate possessed lower IC_{50} value (0.14 μM) in contrast with the unexposed group (8.4 μM) and especially the free cisplatin (16.1 μM).

3. Phototherapy

Phototherapy is an effective cancer therapy that utilizes phototherapeutic agent and photoirradiation at a specific wavelength to induce phototherapeutic effect. It is superior to traditional chemotherapy and radiotherapy by virtue of its non-invasiveness, excellent spatiotemporal controllability, and minimal side effect [38]. Phototherapy includes two major modes: photodynamic therapy (PDT) and photothermal therapy (PTT), each differing in the tumor toxic mechanism. For PDT-mediated phototoxicity, it predominately relies on the generation of reactive oxygen species (ROS), especially singlet oxygen ($^1O_2$), from triplet-triplet annihilation between molecular oxygen ($^3O_2$) and excited triplet photosensitizer (PS) which is converted from excited singlet PS via intersystem crossing (ISC) [39]. Sufficient $^1O_2$* generation can provoke the irreversible destruction of proximal tumor tissues via oxidative damage as well as an immune response against tumor cells and shutdown of tumor-associated vasculature [40]. On the other hand, photothermal agents involved in PTT can convert excitation energy into thermal energy through vibrational relaxation mechanism and elevate local tissue temperature to the clinical hyperthermia range (41 °C–48 °C) or above, leading to irreversible thermoablation of tumor tissues via protein denaturation and coagulative necrosis process [41,42]. Furthermore, the integration of cyanine synergistically combines fluorescence imaging with phototherapy, also termed as phototheranostics. Typically, the “all-in-one” theranostic approach utilizes a single agent for imaging-guided phototherapy by merely imaging and manipulating light irradiation [43].

3.1. Cyanine-based phototherapeutic agents

As mentioned above, some heptamethine cyanine dyes can also act as phototherapeutic agents though possess limited efficacy on account of inherent photophysical and photo-chemical properties. The introduction of heavy atoms into cyanine, e.g., iodination on the heterocyclic nucleus [44], can increase the ISC efficiency and accordingly improve photoconversion efficiency, known as heavy-atom effect. By contrast, a heavy-atom-free cyanine conjugate (**18**) with exceptional singlet oxygen yield, reaching 0.1696 compared to 0.008 of ICG, was recently developed by conjugating with ISC-promoting moiety (Fig. 7A) [45]. Other common limiting factors include short circulation half-life and poor water solubility [8]; encouragingly, numerous research have been dedicated to address these concerns by integrating nanoplatform into these cyanine conjugates (Fig. 7B). Most recently, Leitão et al. reviewed the application of such combination in cancer phototheranostics and mainly focused on IR780, IR808, IR820, IR825 and cypate based nanomaterials [46]. As summarized, loading cyanine photosensitizers into miscellaneous nanostructures remains the

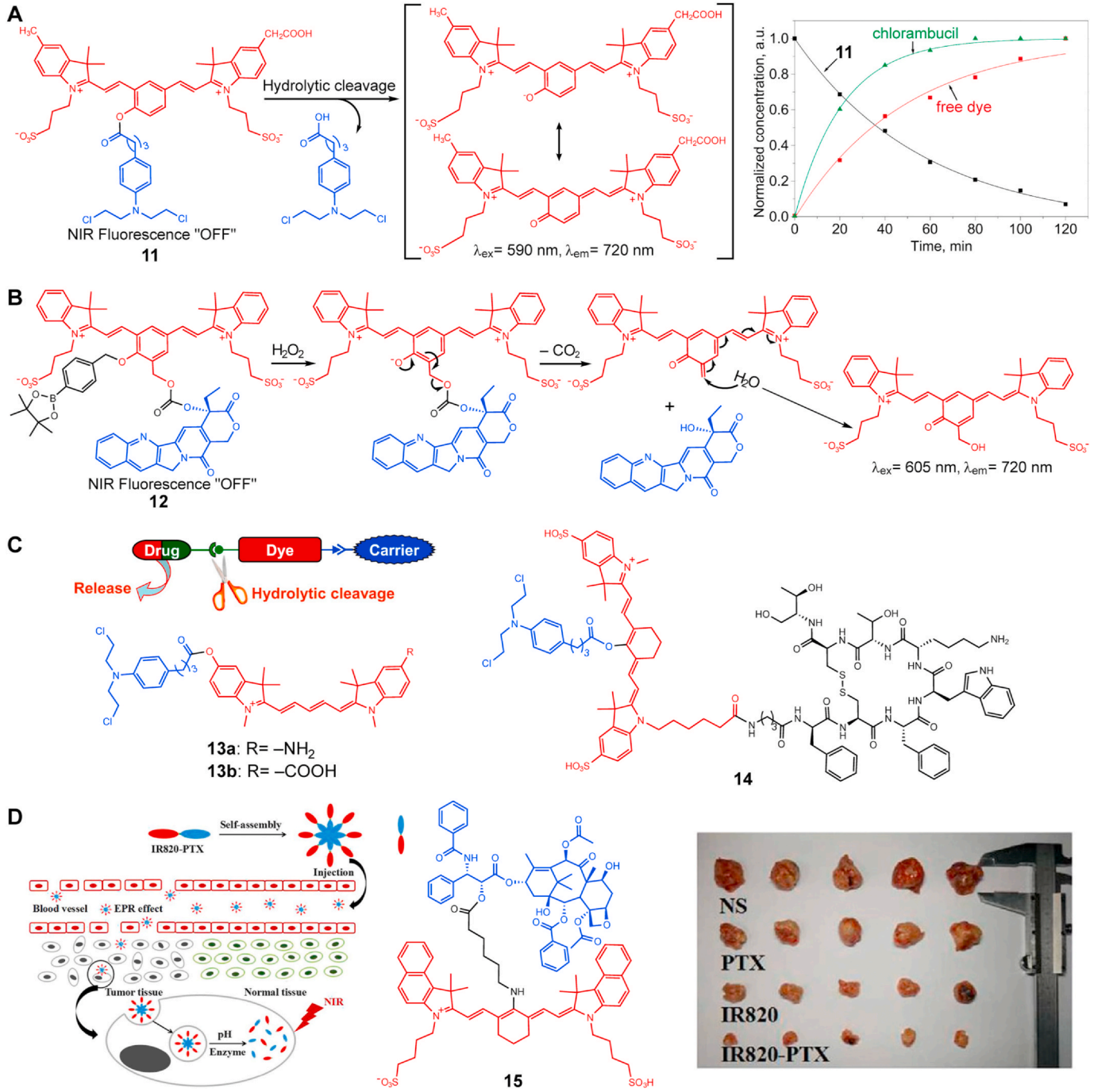

Fig. 5. (A) Cyanine–chlorambucil conjugate **11** with a cleavable phenolic ester linkage and its cleavage profile in phosphate buffer measured by HPLC-MS. Reprinted with permission from Ref. [31]. (B) H_2O_2-triggered cleavage of the phenolic ether and release of camptothecin in conjugate **12**. (C) Design concept of dual-functionalized cyanine scaffold featuring a biodegradable ester bond to release drug, based on which several cyanine conjugates were synthesized (**13–14**). Reprinted with permission from Refs. [33]. (D) Schematic illustration of the self-assembly and cytotoxic mechanism of amphiphilic cyanine conjugate **15** (left). Photographs of the excised tumors after treatment with Normal Saline, PTX, IR820 (λ = 808 nm, P = 1.0 W/cm^2, t = 5 min), and IR820-PTX nanoparticles (λ = 660 nm, P = 1.0 W/cm^2, t = 5 min) (right). Reprinted with permission from Refs. [35].

mainstream methodology. Notably, a subset of cyanine conjugates that could self-assemble into nanoparticles through hydrophobic interaction were reported with improved phototherapeutic efficacy. Typically, the hydrophobic cyanine was conjugated to the terminal of hydrophilic polymer, e.g., the conjugation of $mPEG_{2k}$ and IR780-C13 [47], block copolymer PEG_{5k}-PLD_{10} and IR825 (**19**) [48]; the resultant amphiphilic conjugate then assembled into polymeric micelle in aqueous solution. Interestingly, $mPEG_{2k}$-cypate was decomposed upon NIR irradiation presumably due to the destruction of cypate scaffold, which suggests that such conjugate can be readily degraded after exerting its phototherapeutic effect [49]. Besides, cyanine was conjugated to the internal repeat units of hydrophilic polymer, as is the case for IR808-conjugated biodegradable hyaluronic acid nanoparticles (**20**) [50]. Unlike hydrophobicity-induced assembly, IR820-labeled diblock elastin-like polypeptides (ELP), namely hydrophilic block ELP [$V_1A_8G_7$-32] and zinc ion chelation block ELP [VH_4-40], assembled into a micelle-like nanostructure (**21**) via Zn^{2+}–histidine residue chelation [51]. Another subset of cyanine conjugates were fabricated on nanoparticle cores that

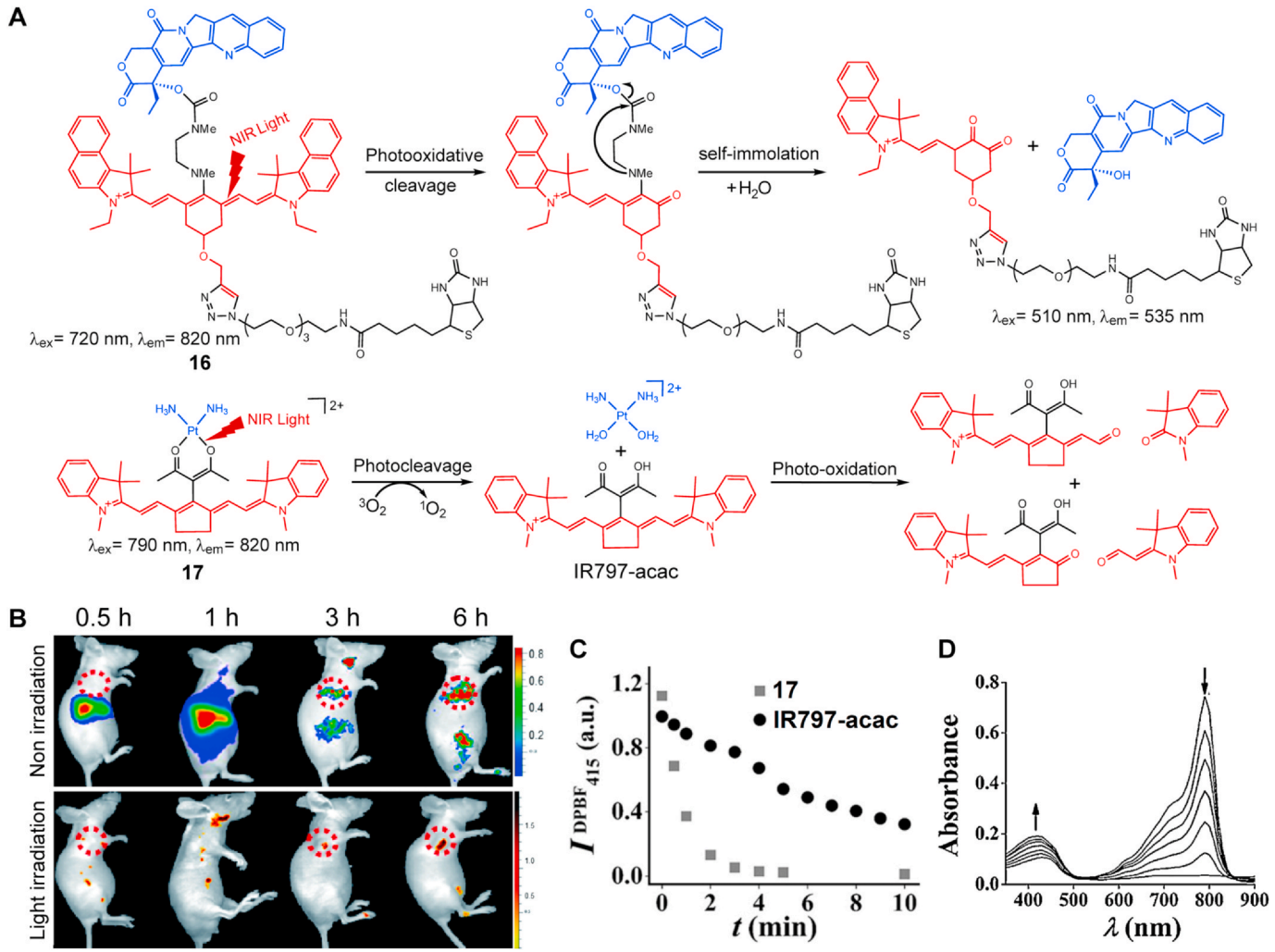

Fig. 6. (A) NIR light – triggered drug release from cyanine conjugates **16–17**. (B) In vivo fluorescence imaging of tumor-bearing mice after intravenous injection of **16** with (535 nm emission) and without (820 nm emission) light irradiation at various time points. Red circle indicated tumor site. Reprinted with permission from Refs. [36]. (C) Scatter plot comparing decrease in absorbance of $^1O_2$ scavenger DPBF at 415 nm in presence of **17** and IR797-acac with time of irradiation in NIR light, showing enhanced $^1O_2$ production after Pt complexation. (D) Absorption spectral of **17** exposed to light (readings at 30 s and 1 min intervals), showing decrease in intensity at 790 nm and increase in intensity at 430 nm. Reprinted with permission from Ref. [37]. (For interpretation of the references to colour in this figure legend, the reader is referred to the Web version of this article.)

function as magnetic resonance imaging (MRI) contrast agents to confer dual-modal imaging capability. Generally, these nanoparticles, including MnO NPs, SPIONPs, $MnFe_2O_4$ NPs, were coated with a layer of polymer (e.g., chitosan quaternary ammonium salt [52], **22**), amphiphilic copolymer (e.g., PSMA-PEG_{2k}-NH_2 [53], **23**) or lipid-polymer (DSPE-PEG_{2k}-NH_2 [54], **24**); subsequently, cyanine photosensitizers were conjugated on the outer surface of polymer. In an innovative biomineralization process, bovine serum albumin was demonstrated to coat gadolinium oxide nanocrystals (GdNCs) and then conjugated with cypate (**25**) [55].

3.2. Cyanine–phototherapeutic agent conjugates

In parallel with exploration of cyanine itself as phototherapeutic agent, efforts dedicated to conjugating cyanine with other phototherapeutic agents are proven practical as well. Pandey's lab conducted a series of research on cyanine conjugates based on 2-(1-hexyloxyethyl)-2-devinyl pyropheophorbide-a (HPPH), a second-generation PS currently in clinical development under the brand name Photochlor® (Fig. 8A). Notably, the minimal overlap of absorption bands between HPPH and cyanine allows for independent fluorescent tracking of the PDT agent without phototoxic consequences. Initially, HPPH was conjugated to IR820 via a short 4-aminophenylthiol linker; though **26** displayed dual-functionality and tumor-avidity, its PDT efficacy was compromised due to the competing förster resonance energy transfer (FRET) process between excited HPPH and cyanine [56]. Thereafter, various HPPH-cyanine conjugates were constructed by altering the cyanine fluorophore, the number of HPPH moiety, the length and orientation of linker and the metalation state of HPPH ring to increase overall singlet oxygen production; and they identified **27–29** with enhanced PDT efficacy in separate work [40,57,58]. Xue and colleagues fabricated a multistep phototherapeutic conjugate (**30**) consisting of a similar photosensitizer pyropheophorbide A (Ppa), Cy7, PEG and tumor-targeting biotin (Fig. 8B) [59]. The linear and amphiphilic conjugate could assemble into nanomicelle for cancer-targeted synergistic PTT/PDT therapy. To be specific, the multistep therapy started from tumor accumulation via EPR and active-targeting effect; upon irradiation of 808 nm laser, Cy7 generated photothermal effect and underwent photodegradation, which collaborately activated the PDT efficacy of Ppa (670 nm). Following this therapeutic regimen, complete tumor ablation was achieved in a mouse xenograft model. Considering the vast diversity of available photosensitizers for PDT, this field remains largely unexplored [60].

Due to the oxygen-dependent characteristic of PDT, its effectiveness

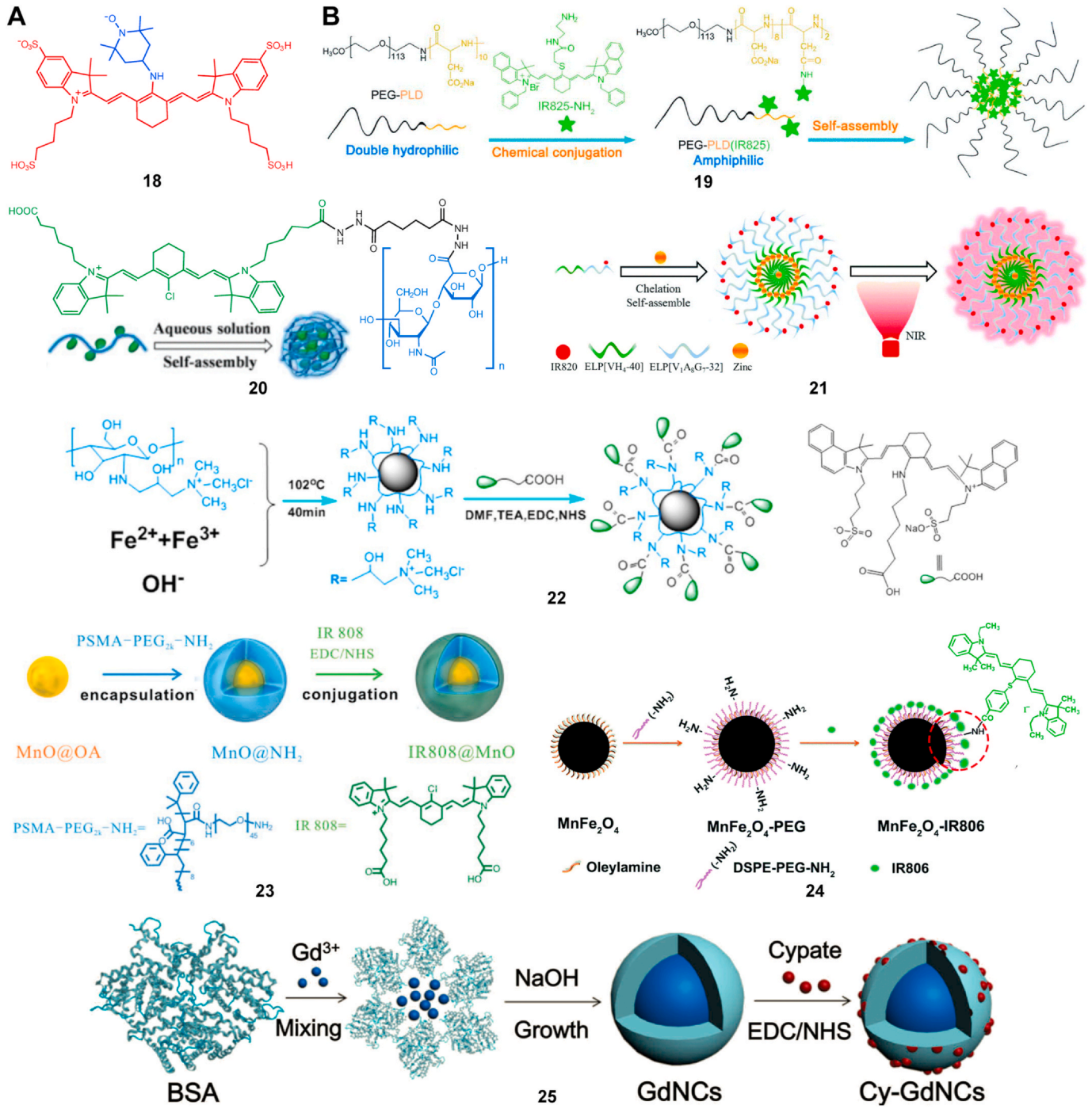

Fig. 7. (A) Cyanine conjugate **18** incorporating an ISC-promoting moiety to enhance singlet oxygen yield. (B) Cyanine conjugates that take advantage of nano-platform to address the inherent limitations of cyanine-based phototherapeutic agents (**19–25**). Reprinted with permission from Refs. [48,50–55].

is inevitably impaired in tumors featuring severe hypoxia. Therefore, PTT may be a potential alternative to PDT in treating hypoxic tumor on account of its oxygen-independent nature. Although a sizable collection of small molecule–based photothermal agents have been developed, their conjugation with cyanine are rarely reported. Regarding nanomaterials-based photothermal agents, the composition, fabrication and function of cyanine conjugates are quiet diverse owing to multifarious nanomaterials and functionalization strategies. Such complexity was best exemplified by Au-based nanomaterials with various morphology, e.g., Au nanorods, Au nanostars, Au nanoclusters. In these conjugates, cyanine fluorophores could be covalently conjugated to Au nanomaterials via Au–S bond [61,62], or indirectly modified through polymer coating [63], complementary base pairing [64] etc.; and many conjugates also exhibited off-on fluorescence/PDT response towards internal stimuli such as pH, GSH, cathepsin E and matrix metalloproteinases (MMPs). A representative cyanine–Au nanorod conjugate **31** was engineered to be a MMPs/pH dual-responsive and pH reversibly activated theranostic platform for fluorescence-guided photothermal therapy (Fig. 8C). Besides, carbon-based nanomaterials were also exploited, including nanographene oxide (NGO) [65] and single-/multi-walled carbon nanotubes (S/M-WNTs) [66,67]. For instance, polyethylene glycol (PEG) and branched polyethylenimine (BPEI) dual-functionalized NGO was utilized to conjugate with IR-808 (**32**) for tumor-targeted imaging and synergistic PDT/PTT (Fig. 8D).

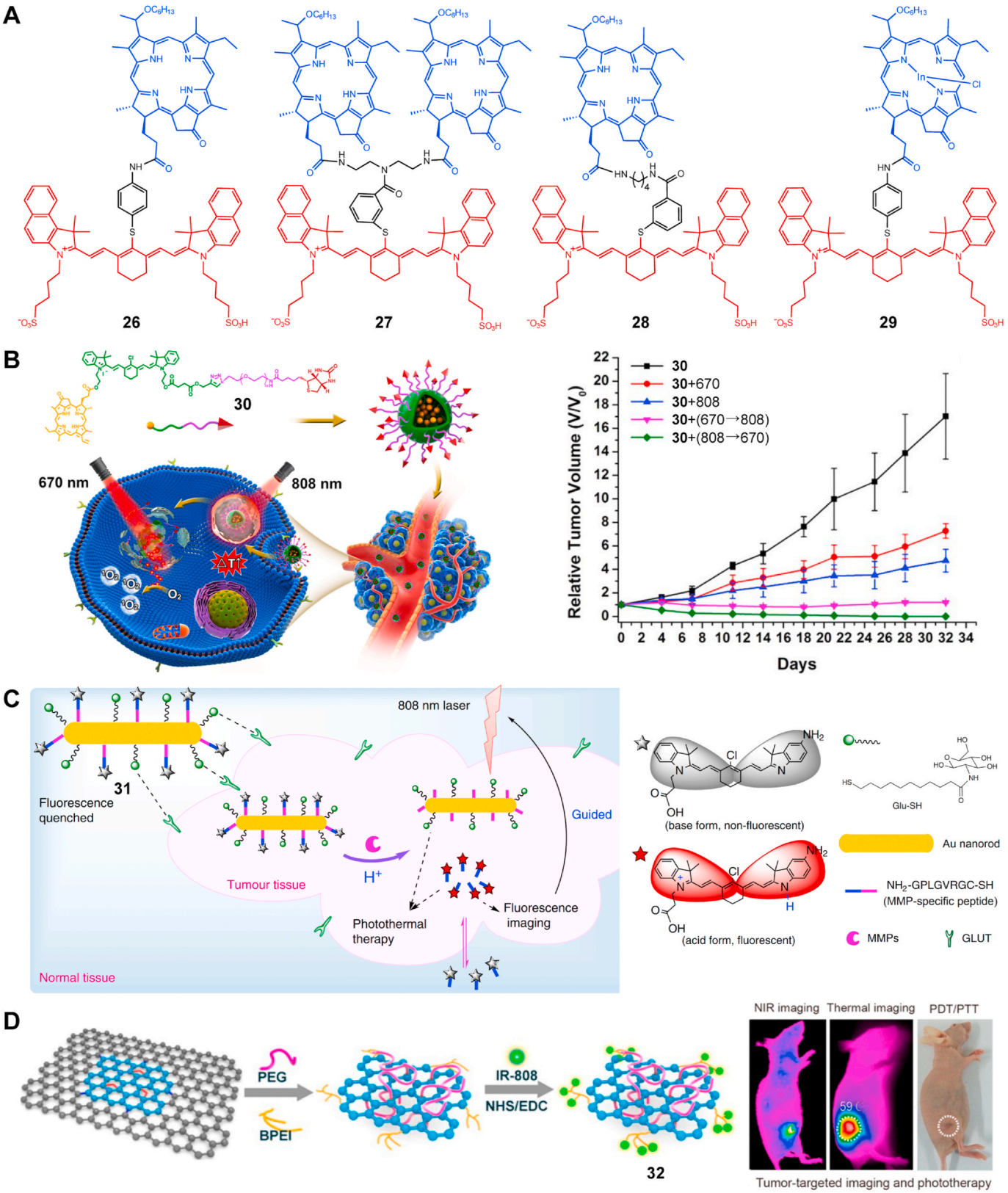

Fig. 8. (A) Cyanine-HPPH conjugates for fluorescence-guided photodynamic therapy (**26–29**). (B) The structure and mechanism of a multistep phototherapeutic conjugate **30** (left). Relative tumor volume curves of mouse xenograft after tail vein injection of this nanomicelles and different laser irradiation regimens (right). Reprinted with permission from Refs. [59]. (C) Schematic illustration of cyanine–Au nanorod conjugate **31** for fluorescence-guided photothermal therapy. Reprinted with permission from Refs. [62]. (D) IR-808 was grafted onto PEG/BPEI dual-functionalized NGO to obtain **32** and representative images showing its utility in tumor-targeted imaging and synergistic phototherapy. Reprinted with permission from Ref. [65].

4. Targeted therapy

Advances in molecular biology and panomics analysis (e.g., genomics, proteomics) have contributed to the identification of miscellaneous molecular targets in cancer cells which are either abnormal or overexpressed compared to normal cells [68]. Rational design of drugs to interfere with these malfunctioning targets should discriminatingly impede tumor progression with less adverse effects, which constitutes the concept of targeted therapy. Up to now, many targets have been validated and harnessed to develop drugs, including transmembrane receptors and intracellular signaling protein kinases in the signal transduction pathways [69]. Currently, there are two main types of targeted therapies: monoclonal antibodies (mAbs) and small molecular inhibitors, which provide two alternatives for cyanine conjugation. Nonetheless, cyanine-mAbs conjugates were mainly reported as fluorescent probes for targeted molecular imaging; its therapeutic effects are somehow dismissed and presumably due to the much lower optimal dose for imaging than for therapeutic purpose. Similarly, another two innovative targeted therapeutic platforms which still remain in early-phase clinical trials, that is, aptamers [70] and non-immunoglobulin protein scaffolds [71], have also been reported to conjugate with cyanine for cancer diagnostic imaging rather than for therapeutic purpose [72,73]. On the other hand, antibody-drug conjugates derived from mAbs were reported to integrate cyanine as theranostic agents.

4.1. Antibody-drug conjugates

Antibody-drug conjugates (ADC), in which antibody serves as targeting warhead for the delivery of chemotherapeutic toxins, is a relatively new class of antibody therapeutics. Generally, the conjugation is accomplished via a linker, either cleavable or non-cleavable; the conjugation chemistry between linker and antibody resembles that of cyanine-antibody conjugates. The linker plays a crucial role in ADC performance and has two fundamental properties: on one hand, it should be stable in systemic circulation to avoid off-target drug release; on the other hand, it needs to be rapidly cleaved upon ADC internalization to release the payload.

Schnermann's lab conducted a pioneering work on integrating cyanine backbone as linker in ADC structure. Moreover, they actualized on-demand drug release through NIR light triggered photooxidative cleavage and successive self-immolation of the caging tether; and such heptamethine cyanine linker could well satisfy the above requirements (Fig. 9A). In the first-generation construct, namely Cy-Pan-CA4 conjugate (**33**), combretastatin A4 (CA4), a potent inhibitor of microtubule polymerization, was employed as toxic payload; and antibody was attached at the carbamate site through Lys–NHS ester chemistry (Fig. 9B) [74]. Notably, panitumumab (Pan), an anti-EGFR mAb, was chosen because EGFR is overexpressed in a subset of NIR accessible cancers, such as head and neck, ovarian, and bladder cancer etc., which holds promise for clinical translation. The conjugate demonstrated favorable merits via in vitro characterization: efficient payload release under irradiation of 690 nm light with minimal background release; similar efficacy compared to free drug and a ~70X therapeutic window (defined as the ratio of unirradiated IC_{50} to irradiated IC_{50}). For in vivo performance, it showed excellent tumor localization and the attenuation of cyanine signal was indicative of drug release. Nevertheless, CA4 is far less potent than typical ADC payloads and thereby is not capable of reducing tumor burden. To this end, they exploited duocarmycin-class payload (Duo) with picomolar potency in the second generation construct, CyEt-Pan-Duo (**34**, Fig. 9C) [75]. Moreover, based on structure-function relationship studies of the caging scaffold, they adopted the N, *N′*-diethylethylenediamine tether and sulfonated benz [*e*]-indole ring to enhance stability, enable higher degree of labeling (~4.0) and red-shift absorption maximum (~40 nm). In concert with these modifications, an alkyne handle was further installed to facilitate antibody bioconjugation. Overall, the conjugate exhibited a 400-fold increase in potency and an 8-fold improvement in therapeutic index compared to Cy-Pan-CA4 [76], and more importantly, inhibited tumor growth under 780 nm light irradiation.

4.2. Small molecular inhibitors

Small molecular inhibitors typically interrupt intracellular signal transduction which initiates a molecular cascade to promote cancer growth, proliferation, metastasis and angiogenesis [77]. The inhibitory effect is primarily caused by occupying the functionally critical domain, usually a well-defined catalytic cleft, of target protein; and its specificity and avidity are also derived from the noncovalent bonding with multiple amino acids residues inside the cleft. For optimal conjugation with cyanine, structural information on the molecular binding mode between inhibitors and target proteins is required to guide the selection of conjugation sites on inhibitors. Moreover, heptamethine cyanine dyes that show preferential tumor accumulation are still beneficial and hence are popularly used.

The majority of small molecular inhibitors target protein kinase, especially tyrosine kinase such as epidermal growth factor receptor (EGFR), vascular endothelial growth factor receptor (VEGFR), and anaplastic lymphoma kinase (ALK) [78]. For example, dasatinib is a clinically available tyrosine kinase inhibitor (TKI) for the treatment of Ph + chronic myelogenous leukemia and acute lymphoblastic leukemia. Recently, Kevin's group reported a cyanine-dasatinib conjugate (**35**), among which MHI-48 was exploited for enhanced tumor delivery (Fig. 10A) [79,80]. Dasatinib targets a panel of tyrosine kinases, including Bcr-Abl and the Src kinase family. And co-crystal structure analysis revealed that the hydroxy group of dasatinib is projected into solvent when in complex with Abl and cSrc, which guided its conjugation with MHI-148 via the –OH group. The binding affinity of **35** was compromised as evidenced by higher IC_{50} values against Src (184 nM) and Lyn (556 nM) relative to that of free drug (12 nM for Src, 18 nM for Lyn). Encouragingly, the conjugate exhibited stronger cytotoxicity than dasatinib, MHI-148, or a mixture of both components in HepG2 cells and U87-MG cells owing to enhanced uptake. In vivo imaging results also showed preferential tumor accumulation but its efficacy was not addressed. Based on similar structure analysis, another TKI crizotinib that targets ALK was conjugated with IR-786 and the piperidine amine served as attachment site (Fig. 10B) [81]. Conjugate **36** displayed an increased anti-proliferative activity (IC_{50} = 4.7 nM) than crizotinib (540 nM) or IR-786 (280 nM) in patient-derived glioblastoma cell lines.

Apart from protein kinase, miscellaneous enzyme targets have been identified for cancer therapy and their corresponding inhibitors are also amenable to conjugating with cyanine. Panobinostat is a potent histone deacetylases (HDAC) inhibitor approved for multiple myeloma treatment and its binding mode with HDAC1 indicates an accessible N atom within the alkyl chain [82]. As determined in HDAC inhibition assay, the cyanine-panobinostat conjugate (**37**) had an IC_{50} value (9.6 nM) comparable to that of free drug. Its tumor-avid property was proven useful in assessing the therapeutic effect of HDAC inhibitor (Fig. 10C). Monoamine oxidase A (MAOA), a conventional target of anti-depressants, is also implicated in prostate cancer. The direct translation of MAOA inhibitor into cancer therapy is impracticable due to its extensive action on central nervous system. A tumor-targeting cyanine dye, MHI-148, was shown to conjugate with two irreversible MAOA inhibitors, i.e., clorgyline (**38**) [83] and isoniazid (**39**) [84], and enhanced their selectivity (Fig. 10D). Instead of directly binding to the active site of target, farnesylthiosalicylic acid (FTS) dislodges chronically active Ras from cellular membrane and hence blocks Ras signaling by mimicking its anchoring moiety. Guan et al. conjugated FTS with tumor-targeting cyanine dye in order to improve its poor pharmacokinetic profile and **40** displayed higher potency than FTS in cellular inhibition assay (Fig. 10D) [85].

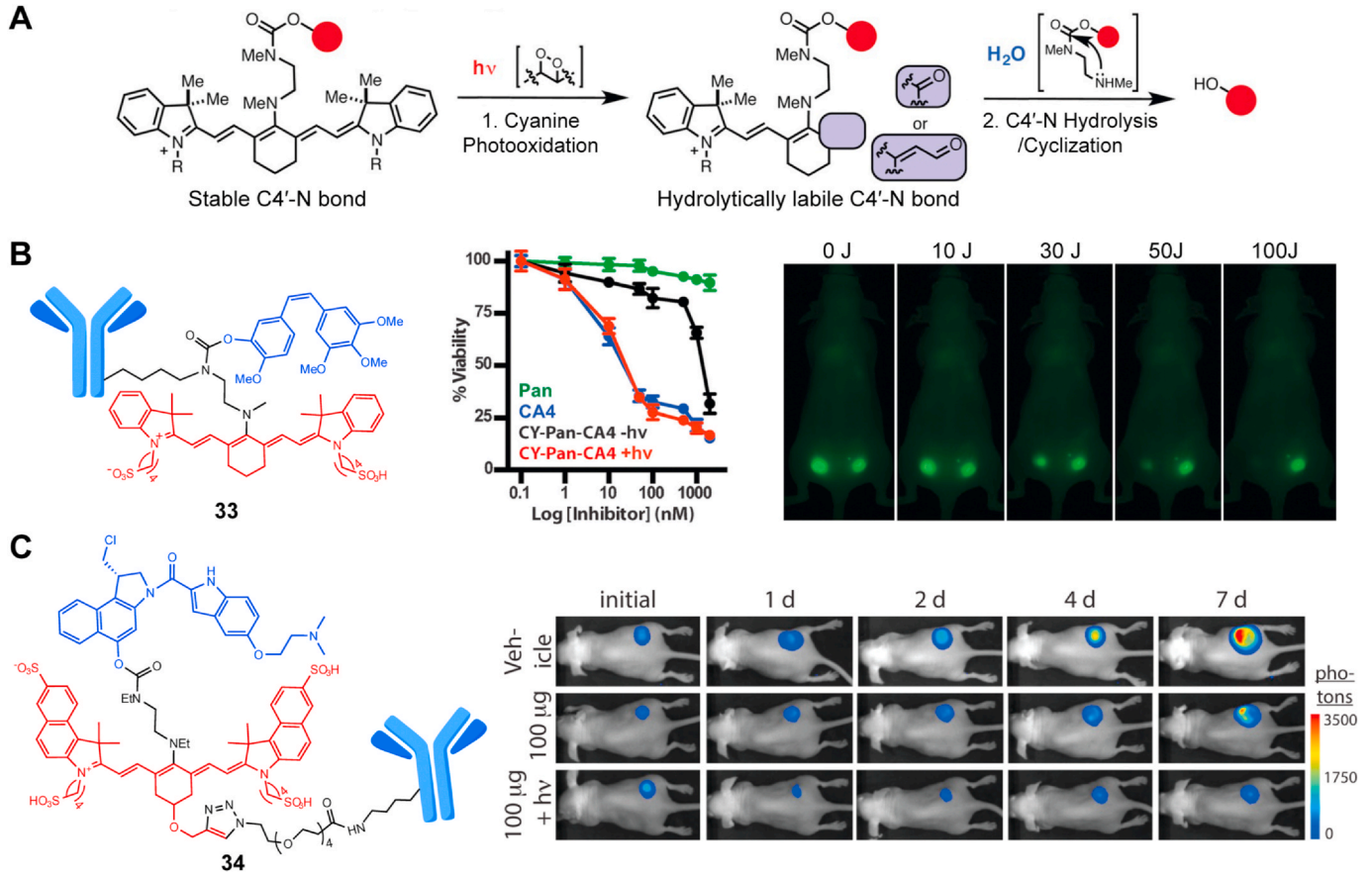

Fig. 9. (A) The mechanism of NIR light triggered drug release from ADC incorporating heptamethine cyanine as linker. (B) The structure of first-generation Cy-Pan-CA4 conjugate (**33**) (left). In vitro light-dependent (690 nm, 30 J) cytotoxicity against MDA-MB-468 cells (middle). In vivo NIRF images of A431 tumors (implanted in both sides of the dorsum) with various doses of 690 nm irradiation only on the left-side tumor at two days post-injection (right). Reprinted with permission from Ref. [74]. (C) The structure of second-generation CyEt-Pan-Duo conjugate (**34**) (left). Bioluminescence images of MDA-MB-468-luc tumor-bearing mice before and after various treatment (right). Reprinted with permission from Ref. [75]. Notice: further permissions related to the material excerpted should be directed to the ACS.

5. Cyanine conjugates as nanocarriers

In contrast to direct conjugation with therapeutic agents, cyanine can be alternatively fabricated into conjugates that function as nanocarriers to deliver therapeutic agents, including chemotherapeutics, gene, etc. [86]. Depending on the structure and composition of nanocarriers, drug can be covalently conjugated, or noncovalently immobilized or encapsulated through electrostatic/hydrophobic interaction. One notable attribute of these nanotherapeutic agents is tumor selectivity, which falls into three mechanisms: passive targeting attributable to the enhanced permeability and retention (EPR) effect, active targeting via targeting ligand–mediated interactions and triggered drug release by intrinsic or extrinsic stimuli [87]. Nevertheless, the toxicity and reproducibility of nanocarrier-based delivery system remain questionable and therefore impede its clinical translation [88,89]. Nanocarriers such as dendrimers, inorganic nanoparticles (e.g., magnetic NPs, gold NPs, silica NPs), polymer-based system (e.g., polymeric NPs, polymeric micelles) and lipid-based system (e.g., liposomes, solid lipid NPs) are common platforms to deliver drugs [90]. The diverse array of nanocarriers provide immense possibility for cyanine conjugation, e.g., surface modification, hydrophobic core. Therefore, for the sake of clarity, we focused on conjugates wherein cyanine plays an indispensable role in the assembly of nanocarrier instead of those obtained through simple modification.

In one approach, cyanine served as a scaffold to link hydrophobic mPEG and hydrophilic poly (*ε*-caprolactone) (PCL) [91]. The mPEG-Cy-PCL conjugate (**41**) could self-assemble into micelle, during which doxorubicin was encapsulated inside the hydrophobic (Fig. 11A). Based on photothermal effect of the cyanine scaffold, this conjugate enabled light-triggered synergistic chemo-photothermal therapy. For hydrophilic drug molecules, a liposome-like bilayer structure is often desirable for efficient loading. Kim and co-workers incorporated a hydrophilic phosphocholine group into the *meso*-site of hydrophobic cyanine dye (**42**) and co-assembled it with PEG-Cy to increase stability and bioavailability (Fig. 11B) [92]. The resultant bilayer nanovesicle could load gemcitabine in its hydrophilic core. In another study, cyanine dyes with different *N*-alkyl side chain length were conjugated with three hydrophilic polymer molecules: one PEG_{5K} and two PEI_{2K} [93]. In aqueous solution, the conjugate with C9 side chain (**43**) adopted a U-shaped configuration and self-assembled into bilayer nanoparticles (Fig. 11C). It could efficiently load methotrexate with an encapsulation efficiency reaching 44.84% and displayed the most pronounced antitumor activity. For tumor targeted gene delivery, Eduardo et al. constructed IR783-b2kPEI conjugate (**44**) as fluorescent nanocarrier, among which the polycationic PEI scaffold was responsible to electrostatically complex with negatively charged nucleic acids (Fig. 11D) [94]. It displayed propitious intracellular transport to the nucleus and was qualified as a tumor-targeted transfection agent with concurrent NIRF signal and gene expression (luciferase) in a mouse xenograft model.

6. Clinical translation

The incentive of conjugation with cyanine is to render drug visible or even controllable and the conjugation with tumor-avid heptamethine cyanine dyes further potentiate the therapeutic effect of small

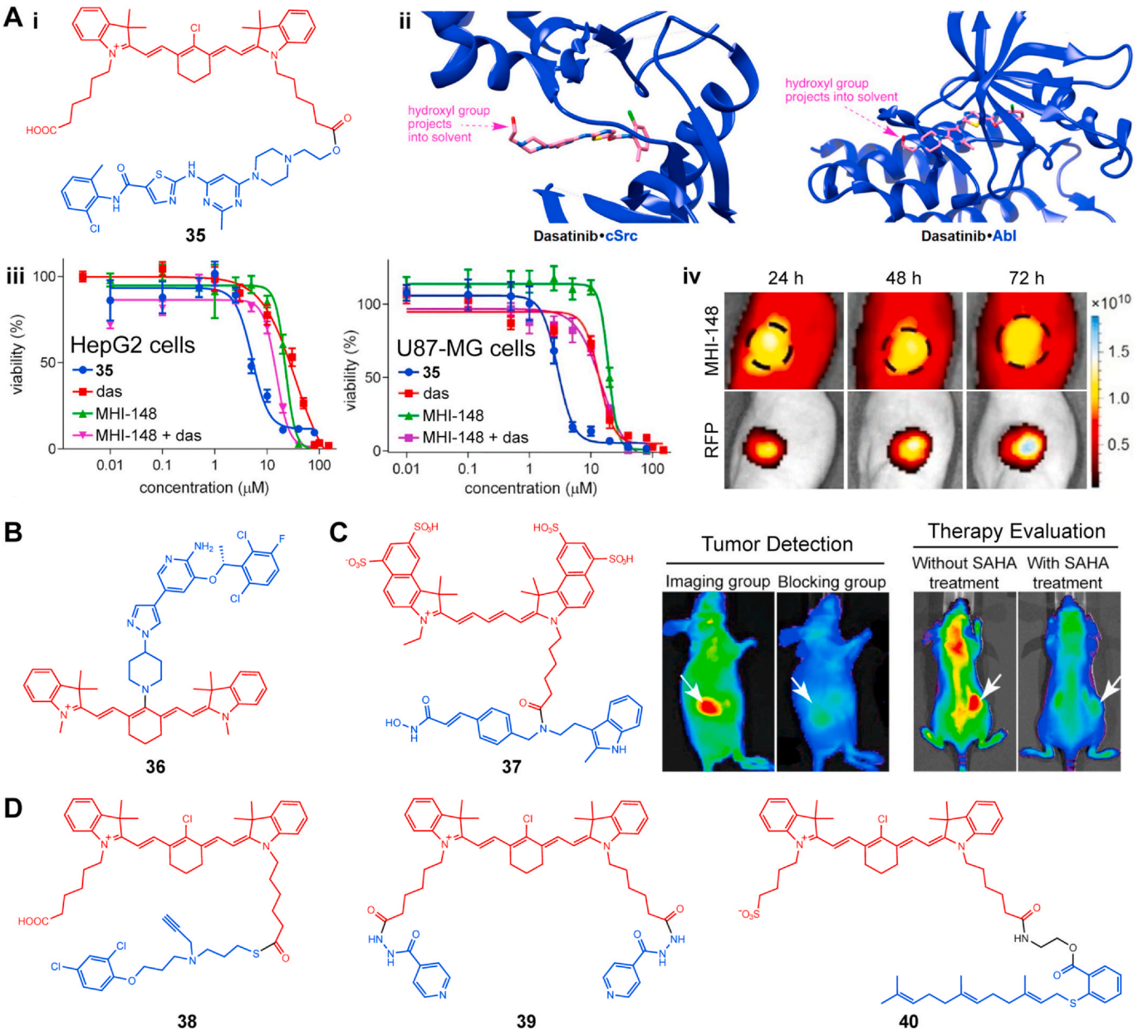

Fig. 10. (A) I, cyanine-dasatinib conjugate **35**. Ii, co-crystal structure analysis of dasatinib with cSrc or Abl. Iii, viabilities of HepG2 or U87-MG cells after incubating with the test compounds for 48 h in the dark. Iv, fluorescence imaging of nude mice implanted with subcutaneous red fluorescence protein (RFP)-expressing U87 glioblastoma tumors at 24, 48, 72 h. Reprinted with permission from Ref. [79,80]. (B) Cyanine-crizotinib conjugate **36**. (C) Cyanine-panobinostat conjugate **37** and its application in tumor detection and HDACi therapy evaluation. Reprinted with permission from Ref. [82] (D) Cyanine conjugates integrating MAOA inhibitor (**38**–**39**) or Ras inhibitor (**40**) as therapeutic agents. (For interpretation of the references to colour in this figure legend, the reader is referred to the Web version of this article.)

molecular drugs. Alternatively, cyanine can be fabricated into conjugates that function as nanocarriers to visualize the delivery process of therapeutic agents or even initiate drug release via photothermal effect.

These two distinct strategies collectively show clinical potential in personalized medicine, in that the therapeutic process–associated information, especially inter-individual heterogeneity in drug metabolism, can be extracted to help adjust the therapeutic regimen. Besides, therapeutic index can be further enhanced owing to cyanine-mediated tumor accumulation and drug activation. Although the above theranostic cyanine conjugates have demonstrated immense potential in preclinical models, none of them have been successfully translated into clinic trials so far.

From a technical perspective, the major obstacle when translating preclinical results into clinical settings is the limited penetration depth of fluorescence imaging accompanied by the remarkable disparity in body size between mouse and human. In preclinical studies, the theranostic capability of cyanine conjugates is generally characterized in subcutaneous xenograft models which may involve subsequent dissection to analyze drug distribution in normal organs and tumors. In clinical settings, however, it only allows to extract minimal diagnostic information from shallow tissue rather than the whole human body as these conjugates are expected to function in a non-invasive manner; therefore, the theranostic value of cyanine conjugates is significantly compromised, especially those aim to extract pharmacokinetic information or monitor activation process. Although technology dedicated to elevate the penetration depth of fluorescence imaging keeps evolving, it is still far from addressing this disparity. On the other hand, seeking for imaging modalities that allow real-time monitoring with

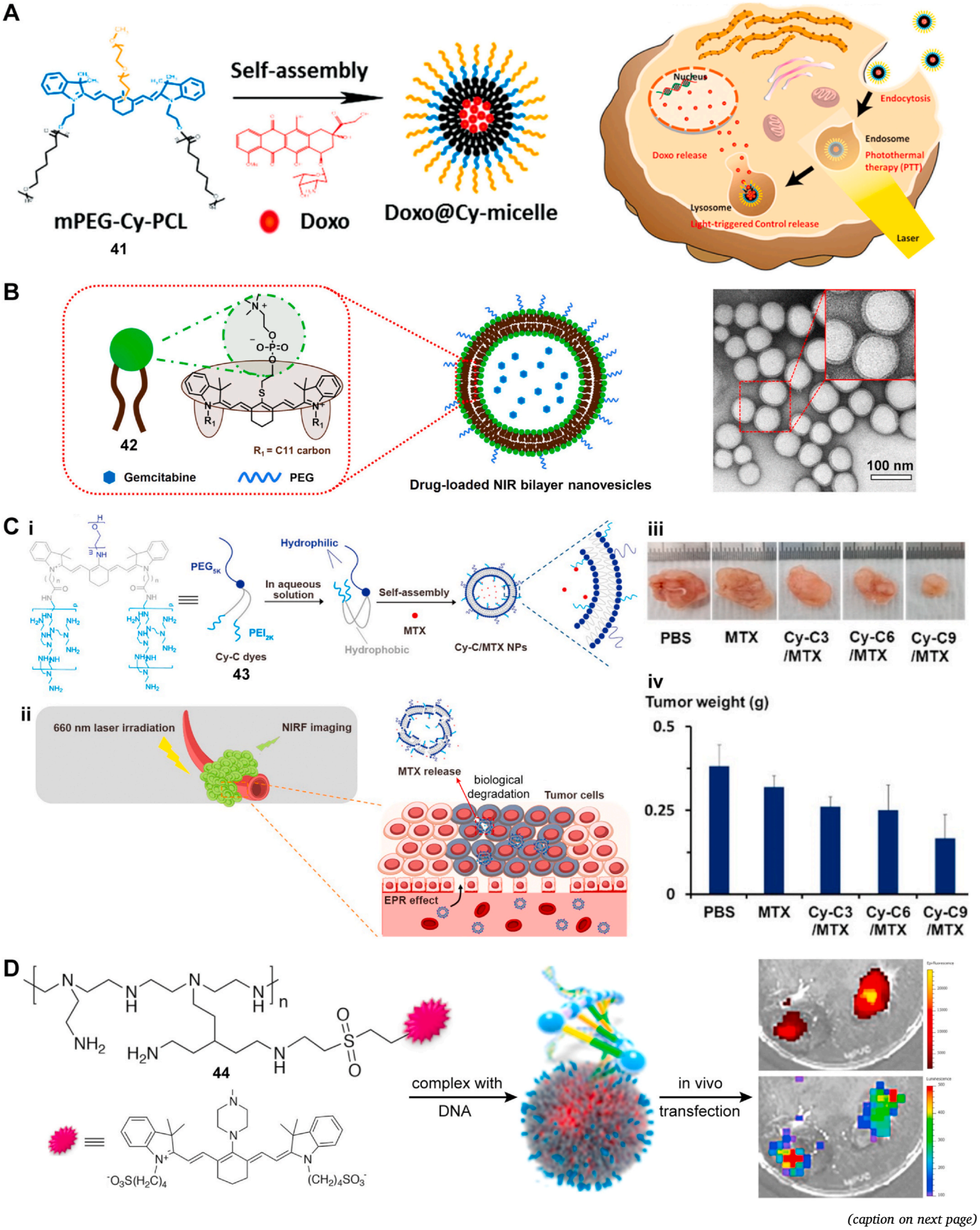

(caption on next page)

Fig. 11. (A) The structure and self-assembly of mPEG-Cy-PCL conjugate **41** (left) and the mechanism of synergistic chemo-photothermal therapy (right). Reprinted with permission from Ref. [91]. (B) Schematic representation of the gemcitabine-loaded bilayer nanovesicles self-assembled from conjugate **42** (left) and TEM images of the empty nanovesicles (right). Reprinted with permission from Ref. [92]. (C) I, the structure and self-assembly of conjugate **43**. Ii, the mechanism of action of methotrexate-loaded bilayer nanoparticles. Iii-iv, representative images of the resected tumor from mouse xenograft models after various treatment and the mean tumor weights of each group (n = 3). Reprinted with permission from Ref. [93]. (D) IR783-b2kPEI conjugate **44** was complexed with luciferase expressing pGL3-control plasmid and used to transfect mice bearing G361 tumor xenograft; NIRF (upper panel) and luminescence (lower panel) imaging of dissected tumors 24 h after intravenous tail injection of the polyplexes. Reprinted with permission from Refs. [94].

desirable penetration depth and can be readily integrated into drugs seems more sensible, yet it is very challenging as well.

Notably, cyanine conjugates that are photoactivatable hold great promise for clinical translation in cancers that are accessible from the surface or endoscopy or fine optical fiber insertion, including head and neck, ovarian, esophagus, bladder, and pancreatic cancer etc. Though the complete diagnostic information is still impossible to acquire, the therapeutic effect can be exquisitely modulated in a spatiotemporal manner and thus it helps to minimize systematic toxicity. For example, cyanine–chemotherapeutic agent conjugates adopting photo-uncaging strategy and ADC drugs that integrate cyanine as photocleavable linker. On the contrary, the translation of nanoparticulate cyanine conjugates confronts additional challenges inherent in nanomedicines, including limited understanding of the biological interaction with human body, safety issues and commercialization hurdles related to large-scale manufacturing and regulatory guidelines [95]. The design guidelines for such nanoparticulate conjugates are as follows: first, choose biocompatible and biodegradable materials, or better, FDA-approved materials, to minimize potential toxicity; second, reduce complexity in formulation design to facilitate reproducible large-scale manufacturing.

7. Conclusion and perspectives

Cyanine is an advantageous fluorogenic unit for the construction of fluorescent probes by virtue of its meritorious attributes, including both favorable fluorescence properties and excellent biocompatibility. Besides, the phototherapeutic potential of several heptamethine cyanine dyes (e.g., IR780, IR820) are explored and these cyanine dyes are qualified as theranostic agents. Previous reviews on the topic of cyanine-based theranostic agents mainly focused on the phototherapeutic effect of cyanine and often involved miscellaneous nanoparticle-based delivery systems. In this review, we highlight the covalent conjugation of cyanine with other therapeutic agents that are commonly utilized in clinics or basic research, including drugs for chemotherapy, phototherapy and targeted therapy. In an additional section, we also introduced cyanine conjugates that function as nanocarriers for the delivery of therapeutic agents. Overall, the therapeutic modality–based classification system clearly demonstrates existing therapeutic agents involved in conjugation and their corresponding conjugation strategies.

The primary thing to consider when designing cyanine–therapeutic agent conjugates is whether the optimal imaging dose of cyanine is within the minimum effective dose and maximum tolerated dose of drug; or they should at least be of the same order of magnitude as the dose ratio can be slightly modified via conjugation chemistry. Additionally, the impact of covalent conjugation on the imaging capability of cyanine and therapeutic effect of drug cannot be underestimated, which may impair such predefined dose compatibility and necessitate comparative study to reconfirm. Sometimes further optimization regarding the structure of cyanine and drug, conjugation site and conjugation chemistry is performed to achieve both satisfactory theranostic capability and acceptable toxicity. For conjugates that serve as nanocarriers, due optimization is needed to balance the equivalent imaging dose of nanoconstruct and the encapsulated drug dose. Nevertheless, most research failed to provide rationale on the dose compatibility and future studies should address this issue in both theoretical and experimental aspects. Secondly, emphasis should be laid on the pharmacokinetic property of cyanine conjugates, particular tumor accumulation capability. Though tumor-avid heptamethine cyanine and EPR effect of nanoparticulate conjugates are beneficial, the conjugation with targeting ligands can further enhance cancer targeting effect through different mechanisms.

As mentioned in the above section, the limited penetration depth of fluorescence imaging diminishes the diagnostic value of most cyanine conjugates and thus poses a formidable challenge for clinical translation. Therefore, it is necessary to identify the most promising directions and ultimately, to establish the clinical value of this research field. Besides, the poor photostability of cyanine precludes real-time monitoring for long periods of time and rather makes it more amenable to imaging at serial time points. Other limitations exist in the methodology that is commonly used for in vivo evaluation in current research. First, the subcutaneous mouse xenograft models are incompetent to imitate the complexity and heterogeneity of human tumors, and the theranostic procedure performed on humans. Thereby, patient-derived xenograft models, orthotopic tumor models, and large animals are recommended for future research. Second, the utility of planar fluorescence imaging is compromised by information deficiency in the z-axis; and more advanced imaging technology is warranted to address this issue. Take a preclinical multi-modality in vivo imaging platform FLECT/CT (fluorescence emission computed tomography/computed tomography) for example, it acquires both CT and fluorescence data for complete angle 3D tomographic imaging and hence maximizes the information attained in a single imaging session.

Declaration of competing interest

None.

Declaration of competing interest

All authors declare that there are no actual or potential competing financial interests.

Acknowledgments

This contribution was financially supported by National Key Research and Development Program of China (No. 2016YFA0201400), State Key Program of National Natural Science of China (No. 81930047), Projects of International Cooperation and Exchanges NSFC-PSF (No. 31961143003), National Project for Research and Development of Major Scientific Instruments (No. 81727803), Beijing Natural Science Foundation, Haidian, original innovation joint fund (No. 17L20170), and the Foundation for Innovative Research Groups of the National Natural Science Foundation of China (No. 81421004).

References

[1] R. Kumar, W.S. Shin, K. Sunwoo, W.Y. Kim, S. Koo, S. Bhuniya, J.S. Kim, Small conjugate-based theranostic agents: an encouraging approach for cancer therapy, Chem. Soc. Rev. 44 (2015) 6670–6683, https://doi.org/10.1039/c5cs00224a.

[2] R. Kojima, D. Aubel, M. Fussenegger, Novel theranostic agents for next-generation personalized medicine: small molecules, nanoparticles, and engineered mammalian cells, Curr. Opin. Chem. Biol. 28 (2015) 29–38, https://doi.org/10.1016/j.cbpa.2015.05.021.

[3] A. Mishra, R.K. Behera, P.K. Behera, B.K. Mishra, G.B. Behera, Cyanines during the 1990s: A review, Chem. Rev. 100 (2000) 1973–2012, https://doi.org/10.1021/cr990402t.

[4] H.A. Shindy, Basics, mechanisms and properties in the chemistry of cyanine dyes: a

review paper, Mini-Reviews Org. Chem. 9 (2012) 352–360, https://doi.org/10.2174/157019312804699528.
[5] M. Fang, S. Xia, J. Bi, T. Wigstrom, L. Valenzano, J. Wang, W. Mazi, M. Tanasova, F. Luo, H. Liu, A cyanine-based fluorescent cassette with aggregation-induced emission for sensitive detection of pH changes in live cells, Chem. Commun. 54 (2018) 1133–1136, https://doi.org/10.1039/c7cc08986d.
[6] L. Gui, Z. Yuan, H. Kassaye, J. Zheng, Y. Yao, F. Wang, Q. He, Y. Shen, L. Liang, H. Chen, A tumor-targeting probe based on a mitophagy process for live imaging, Chem. Commun. 54 (2018) 9675–9678, https://doi.org/10.1039/c8cc04246b.
[7] R. Liu, J. Tang, Y. Xu, Z. Dai, Bioluminescence imaging of inflammation in vivo based on bioluminescence and fluorescence resonance energy transfer using nanobubble ultrasound contrast agent, ACS Nano 13 (2019) 5124–5132, https://doi.org/10.1021/acsnano.8b08359.
[8] S. Hameed, H. Chen, M. Irfan, S.Z. Bajwa, W.S. Khan, S.M. Baig, Z. Dai, Fluorescence guided sentinel lymph node mapping: from current molecular probes to future multimodal nanoprobes, Bioconjugate Chem. 30 (2019) 13–28, https://doi.org/10.1021/acs.bioconjchem.8b00812.
[9] M. Kaur, D.H. Choi, Diketopyrrolopyrrole: brilliant red pigment dye-based fluorescent probes and their applications, Chem. Soc. Rev. 44 (2015) 58–77, https://doi.org/10.1039/c4cs00248b.
[10] Q. You, Q. Sun, J. Wang, X. Tan, X. Pang, L. Liu, M. Yu, F. Tan, N. Li, A single-light triggered and dual-imaging guided multifunctional platform for combined photothermal and photodynamic therapy based on TD-controlled and ICG-loaded CuS@mSiO, Nanoscale 9 (2017) 3784–3796, https://doi.org/10.1039/c6nr09042g.
[11] S. Luo, E. Zhang, Y. Su, T. Cheng, C. Shi, A review of NIR dyes in cancer targeting and imaging, Biomaterials 32 (2011) 7127–7138, https://doi.org/10.1016/j.biomaterials.2011.06.024.
[12] J.O. Escobedo, O. Rusin, S. Lim, R.M. Strongin, NIR dyes for bioimaging applications, Curr. Opin. Chem. Biol. 14 (2010) 64–70, https://doi.org/10.1016/j.cbpa.2009.10.022.
[13] P.J. Choi, T.I.H. Park, E. Cooper, M. Dragunow, W.A. Denny, J. Jose, Heptamethine cyanine dye mediated drug delivery: hype or hope, Bioconjugate Chem. 31 (2020) 1724–1739, https://doi.org/10.1021/acs.bioconjchem.0c00302.
[14] S.M. Usama, C.M. Lin, K. Burgess, On the mechanisms of uptake of tumor-seeking cyanine dyes, Bioconjugate Chem. 29 (2018) 3886–3895, https://doi.org/10.1021/acs.bioconjchem.8b00708.
[15] S.M. Usama, G.K. Park, S. Nomura, Y. Baek, H.S. Choi, K. Burgess, Role of albumin in accumulation and persistence of tumor-seeking cyanine dyes, Bioconjugate Chem. 31 (2020) 248–259, https://doi.org/10.1021/acs.bioconjchem.9b00771.
[16] R.G. Thomas, Y.Y. Jeong, NIRF heptamethine cyanine dye nanocomplexes for multi modal theranosis of tumors, Chonnam Med. J. 53 (2017) 83–94, https://doi.org/10.4068/cmj.2017.53.2.83.
[17] P. Bhattarai, Z. Dai, Cyanine based nanoprobes for cancer theranostics, Adv. Healthcare Mater. 6 (2017) e1700262, , https://doi.org/10.1002/adhm.201700262.
[18] J.A. McKnight, Principles of chemotherapy, Clin. Tech. Small Anim. Pract. 18 (2003) 67–72, https://doi.org/10.1053/svms.2003.36617.
[19] J.B. Wu, C. Shi, G.C. Chu, Q. Xu, Y. Zhang, Q. Li, J.S. Yu, H.E. Zhau, L.W. Chung, Near-infrared fluorescence heptamethine carbocyanine dyes mediate imaging and targeted drug delivery for human brain tumor, Biomaterials 67 (2015) 1–10, https://doi.org/10.1016/j.biomaterials.2015.07.028.
[20] Z. Jiang, K. Pflug, S.M. Usama, D. Kuai, X. Yan, R. Sitcheran, K. Burgess, Cyanine-gemcitabine conjugates as targeted theranostic agents for glioblastoma tumor cells, J. Med. Chem. 62 (2019) 9236–9245, https://doi.org/10.1021/acs.jmedchem.9b01147.
[21] X. Zhang, N. Zhao, B. Wang, Z. Tian, Y. Dai, P. Ning, D. Chen, Structure-inherent near-infrared fluorescent probe mediates apoptosis imaging and targeted drug delivery in vivo, Dyes Pigments 138 (2017) 204–212, https://doi.org/10.1016/j.dyepig.2016.11.022.
[22] E. Zhang, S. Luo, X. Tan, C. Shi, Mechanistic study of IR-780 dye as a potential tumor targeting and drug delivery agent, Biomaterials 35 (2014) 771–778, https://doi.org/10.1016/j.biomaterials.2013.10.033.
[23] Y. Guan, Y. Zhang, J. Zou, L.P. Huang, M.D. Chordia, W. Yue, J.J. Wu, D.F. Pan, Synthesis and biological evaluation of genistein-IR783 conjugate: cancer cell targeted delivery in MCF-7 for superior anti-cancer therapy, Molecules 24 (2019) 4120, https://doi.org/10.3390/molecules24224120.
[24] D. Komljenovic, M. Wiessler, W. Waldeck, V. Ehemann, R. Pipkorn, H.-H. Schrenk, J. Debus, K. Braun, NIR-cyanine dye linker: a promising candidate for isochronic fluorescence imaging in molecular cancer diagnostics and therapy monitoring, Theranostics 6 (2016) 131–141, https://doi.org/10.7150/thno.11460.
[25] C.S. Kang, S. Ren, X. Sun, H.S. Chong, Theranostic polyaminocarboxylate-cyanine-transferrin conjugate for anticancer therapy and near-infrared optical imaging, ChemMedChem 11 (2016) 2188–2193, https://doi.org/10.1002/cmdc.201600072.
[26] S. Mo, X. Zhang, S. Hameed, Y. Zhou, Z. Dai, Glutathione-responsive disassembly of disulfide dicyanine for tumor imaging with reduction in background signal intensity, Theranostics 10 (2020) 2130–2140, https://doi.org/10.7150/thno.39673.
[27] S. Li, Z. Sun, X. Meng, G. Deng, J. Zhang, K. Zhou, W. Li, L. Zhou, P. Gong, L. Cai, Targeted methotrexate prodrug conjugated with heptamethine cyanine dye improving chemotherapy and monitoring itself activating by dual-modal imaging, Front. Mater. 5 (2018) 35, https://doi.org/10.3389/fmats.2018.00035.
[28] M. Ye, X. Wang, J. Tang, Z. Guo, Y. Shen, H. Tian, W.-H. Zhu, Dual-channel NIR activatable theranostic prodrug for in vivo spatiotemporal tracking thiol-triggered chemotherapy, Chem. Sci. 7 (2016) 4958–4965, https://doi.org/10.1039/c6sc00970k.
[29] Y. Zhang, Q. Yin, J. Yen, J. Li, H. Ying, H. Wang, Y. Hua, E.J. Chaney, S.A. Boppart, J. Cheng, Non-invasive, real-time reporting drug release in vitro and in vivo, Chem. Commun. 51 (2015) 6948–6951, https://doi.org/10.1039/c4cc09920f.
[30] Z. Yang, J.H. Lee, H.M. Jeon, J.H. Han, N. Park, Y. He, H. Lee, K.S. Hong, C. Kang, J.S. Kim, Folate-based near-infrared fluorescent theranostic gemcitabine delivery, J. Am. Chem. Soc. 135 (2013) 11657–11662, https://doi.org/10.1021/ja405372k.
[31] M. Bokan, G. Gellerman, L.D. Patsenker, Drug delivery platform comprising long-wavelength fluorogenic phenolo-cyanine dye for real-time monitoring of drug release, Dyes Pigments 171 (2019) 107703, , https://doi.org/10.1016/j.dyepig.2019.107703.
[32] O. Redy-Keisar, S. Ferber, R. Satchi-Fainaro, D. Shabat, NIR fluorogenic dye as a modular platform for prodrug assembly: real-time in vivo monitoring of drug release, ChemMedChem 10 (2015) 999–1007, https://doi.org/10.1002/cmdc.201500060.
[33] A. Rozovsky, L. Patsenker, G. Gellerman, Bifunctional reactive pentamethine cyanine dyes for biomedical applications, Dyes Pigments 162 (2019) 18–25, https://doi.org/10.1016/j.dyepig.2018.09.064.
[34] A. Rozovsky, T.M. Ebaston, A. Zaporozhets, A. Bazylevich, H. Tuchinsky, L. Patsenker, G. Gellerman, Theranostic system for ratiometric fluorescence monitoring of peptide-guided targeted drug delivery, RSC Adv. 9 (2019) 32656–32664, https://doi.org/10.1039/c9ra06334j.
[35] D. Zhang, J. Zhang, Q. Li, H. Tian, N. Zhang, Z. Li, Y. Luan, pH- and enzyme-sensitive IR820-paclitaxel conjugate self-assembled nanovehicles for near-infrared fluorescence imaging-guided chemo-photothermal therapy, ACS Appl. Mater. Interfaces 10 (2018) 30092–30102, https://doi.org/10.1021/acsami.8b09098.
[36] Z. Guo, Y. Ma, Y. Liu, C. Yan, P. Shi, H. Tian, W.-H. Zhu, Photocaged prodrug under NIR light-triggering with dual-channel fluorescence: in vivo real-time tracking for precise drug delivery, Sci. China Chem. 61 (2018) 1293–1300, https://doi.org/10.1007/s11426-018-9240-6.
[37] K. Mitra, C.E. Lyons, M.C.T. Hartman, A platinum(II) complex of heptamethine cyanine for photoenhanced cytotoxicity and cellular imaging in near-IR light, Angew. Chem. Int. Ed. 57 (2018) 10263–10267, https://doi.org/10.1002/anie.201806911.
[38] L. Ricciardi, L. Sancey, G. Palermo, R. Termine, A. De Luca, E.I. Szerb, I. Aiello, M. Ghedini, G. Strangi, M. La Deda, Plasmon-mediated cancer phototherapy: the combined effect of thermal and photodynamic processes, Nanoscale 9 (2017) 19279–19289, https://doi.org/10.1039/c7nr05522f.
[39] Y. You, X. Liang, T. Yin, M. Chen, C. Qiu, C. Gao, X. Wang, Y. Mao, E. Qu, Z. Dai, R. Zheng, Porphyrin-grafted lipid microbubbles for the enhanced efficacy of photodynamic therapy in prostate cancer through ultrasound-controlled in situ accumulation, Theranostics 8 (2018) 1665–1677, https://doi.org/10.7150/thno.22469.
[40] N.S. James, T.Y. Ohulchanskyy, Y. Chen, P. Joshi, X. Zheng, L.N. Goswami, R.K. Pandey, Comparative tumor imaging and PDT Efficacy of HPPH conjugated in the mono- and di-forms to various polymethine cyanine dyes: part - 2, Theranostics 3 (2013) 703–718, https://doi.org/10.7150/thno.5923.
[41] K.K. Ng, G. Zheng, Molecular interactions in organic nanoparticles for phototheranostic applications, Chem. Rev. 115 (2015) 11012–11042, https://doi.org/10.1021/acs.chemrev.5b00140.
[42] D. Jaque, L. Martínez Maestro, B. del Rosal, P. Haro-Gonzalez, A. Benayas, J.L. Plaza, E. Martín Rodríguez, J. García Solé, Nanoparticles for photothermal therapies, Nanoscale 6 (2014) 9494–9530, https://doi.org/10.1039/c4nr00708e.
[43] A. Sahu, J. Lee, H. Lee, Y. Jeong, G. Tae, Prussian blue/serum albumin/indocyanine green as a multifunctional nanotheranostic agent for bimodal imaging guided laser mediated combinatorial phototherapy, J. Contr. Release 236 (2016) 90–99, https://doi.org/10.1016/j.jconrel.2016.06.031.
[44] J. Atchison, S. Kamila, H. Nesbitt, K.A. Logan, D.M. Nicholas, C. Fowley, J. Davis, B. Callan, A.P. McHale, J.F. Callan, Iodinated cyanine dyes: a new class of sensitisers for use in NIR activated photodynamic therapy (PDT), Chem. Commun. 53 (2017) 2009–2012, https://doi.org/10.1039/c6cc09624g.
[45] X. Yang, J. Bai, Y. Qian, The investigation of unique water-soluble heptamethine cyanine dye for use as NIR photosensitizer in photodynamic therapy of cancer cells, Spectrochim. Acta, Part A 228 (2020) 117702, , https://doi.org/10.1016/j.saa.2019.117702.
[46] M.M. Leitao, D. de Melo-Diogo, C.G. Alves, R. Lima-Sousa, I.J. Correia, Prototypic heptamethine cyanine incorporating nanomaterials for cancer phototheragnostic, Adv. Healthcare Mater. 9 (2020) e1901665, , https://doi.org/10.1002/adhm.201901665.
[47] A. Yuan, X. Qiu, X. Tang, W. Liu, J. Wu, Y. Hu, Self-assembled PEG-IR-780-C13 micelle as a targeting, safe and highly-effective photothermal agent for in vivo imaging and cancer therapy, Biomaterials 51 (2015) 184–193, https://doi.org/10.1016/j.biomaterials.2015.01.069.
[48] G.Y. Pan, H.R. Jia, Y.X. Zhu, F.G. Wu, Turning double hydrophilic into amphiphilic: IR825-conjugated polymeric nanomicelles for near-infrared fluorescence imaging-guided photothermal cancer therapy, Nanoscale 10 (2018) 2115–2127, https://doi.org/10.1039/c7nr07495f.
[49] W. Miao, H. Kim, V. Gujrati, J.Y. Kim, H. Jon, Y. Lee, M. Choi, J. Kim, S. Lee, D.Y. Lee, S. Kang, S. Jon, Photo-decomposable organic nanoparticles for combined tumor optical imaging and multiple phototherapies, Theranostics 6 (2016) 2367–2379, https://doi.org/10.7150/thno.15829.
[50] S. Li, Z. Sun, G. Deng, X. Meng, W. Li, D. Ni, J. Zhang, P. Gong, L. Cai, Dual-modal imaging-guided highly efficient photothermal therapy using heptamethine cyanine-conjugated hyaluronic acid micelles, Biomater. Sci. 5 (2017) 1122–1129, https://doi.org/10.1039/c7bm00230k.
[51] K. Huang, M. Gao, L. Fan, Y. Lai, H. Fan, Z. Hua, IR820 covalently linked with self-assembled polypeptide for photothermal therapy applications in cancer, Biomater. Sci. 6 (2018) 2925–2931, https://doi.org/10.1039/c8bm00399h.
[52] H. Zhou, X. Hou, Y. Liu, T. Zhao, Q. Shang, J. Tang, J. Liu, Y. Wang, Q. Wu, Z. Luo, H. Wang, C. Chen, Superstable magnetic nanoparticles in conjugation with near-

infrared dye as a multimodal theranostic platform, ACS Appl. Mater. Interfaces 8 (2016) 4424–4433, https://doi.org/10.1021/acsami.5b11308.
[53] L. Zhou, Y. Wu, X. Meng, S. Li, J. Zhang, P. Gong, P. Zhang, T. Jiang, G. Deng, W. Li, Z. Sun, L. Cai, Dye-anchored MnO nanoparticles targeting tumor and inducing enhanced phototherapy effect via mitochondria-mediated pathway, Small 14 (2018) e1801008, , https://doi.org/10.1002/smll.201801008.
[54] K. Deng, Y. Chen, C. Li, X. Deng, Z. Hou, Z. Cheng, Y. Han, B. Xing, J. Lin, 808 nm light responsive nanotheranostic agents based on near-infrared dye functionalized manganese ferrite for magnetic-targeted and imaging-guided photodynamic/photothermal therapy, J. Mater. Chem. B 5 (2017) 1803–1814, https://doi.org/10.1039/c6tb03233h.
[55] Y. Wang, T. Yang, H. Ke, A. Zhu, Y. Wang, J. Wang, J. Shen, G. Liu, C. Chen, Y. Zhao, H. Chen, Smart albumin-biomineralized nanocomposites for multimodal imaging and photothermal tumor ablation, Adv. Mater. 27 (2015) 3874–3882, https://doi.org/10.1002/adma.201500229.
[56] Y. Chen, A. Gryshuk, S. Achilefu, T. Ohulchansky, W. Potter, T. Zhong, J. Morgan, B. Chance, P.N. Prasad, B.W. Henderson, A. Oseroff, R.K. Pandey, A novel approach to a bifunctional photosensitizer for tumor imaging and phototherapy, Bioconjugate Chem. 16 (2005) 1264–1274, https://doi.org/10.1021/bc050177o.
[57] N.J. Patel, Y. Chen, P. Joshi, P. Pera, H. Baumann, J.R. Missert, K. Ohkubo, S. Fukuzumi, R.R. Nani, M.J. Schnermann, P. Chen, J. Zhu, K.M. Kadish, R.K. Pandey, Effect of metalation on porphyrin-based bifunctional agents in tumor imaging and photodynamic therapy, Bioconjugate Chem. 27 (2016) 667–680, https://doi.org/10.1021/acs.bioconjchem.5b00656.
[58] N.S. James, P. Joshi, T.Y. Ohulchanskyy, Y. Chen, W. Tabaczynski, F. Durrani, M. Shibata, R.K. Pandey, Photosensitizer (PS)-cyanine dye (CD) conjugates: impact of the linkers joining the PS and CD moieties and their orientation in tumor-uptake and photodynamic therapy (PDT), Eur. J. Med. Chem. 122 (2016) 770–785, https://doi.org/10.1016/j.ejmech.2016.06.045.
[59] Y. Xue, J. Li, G. Yang, Z. Liu, H. Zhou, W. Zhang, Multistep consolidated phototherapy mediated by a NIR-activated photosensitizer, ACS Appl. Mater. Interfaces 11 (2019) 33628–33636, https://doi.org/10.1021/acsami.9b10605.
[60] M. Lan, S. Zhao, W. Liu, C.S. Lee, W. Zhang, P. Wang, Photosensitizers for photodynamic therapy, Adv. Healthcare Mater. 8 (2019) e1900132, , https://doi.org/10.1002/adhm.201900132.
[61] H. Li, P. Wang, Y. Deng, M. Zeng, Y. Tang, W.H. Zhu, Y. Cheng, Combination of active targeting, enzyme-triggered release and fluorescent dye into gold nanoclusters for endomicroscopy-guided photothermal/photodynamic therapy to pancreatic ductal adenocarcinoma, Biomaterials 139 (2017) 30–38, https://doi.org/10.1016/j.biomaterials.2017.05.030.
[62] X. Zhao, C.X. Yang, L.G. Chen, X.P. Yan, Dual-stimuli responsive and reversibly activatable theranostic nanoprobe for precision tumor-targeting and fluorescence-guided photothermal therapy, Nat. Commun. 8 (2017) 14998, https://doi.org/10.1038/ncomms14998.
[63] M. Lu, N. Kang, C. Chen, L. Yang, Y. Li, M. Hong, X. Luo, L. Ren, X. Wang, Plasmonic enhancement of cyanine dyes for near-infrared light-triggered photodynamic/photothermal therapy and fluorescent imaging, Nanotechnology 28 (2017) 445710, https://doi.org/10.1088/1361-6528/aa81e1.
[64] R. Yan, J. Chen, J. Wang, J. Rao, X. Du, Y. Liu, L. Zhang, L. Qiu, B. Liu, Y.D. Zhao, P. Jiang, C. Chen, Y.Q. Li, A nanoflare-based strategy for in situ tumor margin demarcation and neoadjuvant gene/photothermal therapy, Small 14 (2018) e1802745, , https://doi.org/10.1002/smll.201802745.
[65] S. Luo, Z. Yang, X. Tan, Y. Wang, Y. Zeng, Y. Wang, C. Li, R. Li, C. Shi, Multifunctional photosensitizer grafted on polyethylene glycol and polyethylenimine dual-functionalized nanographene oxide for cancer-targeted near-infrared imaging and synergistic phototherapy, ACS Appl. Mater. Interfaces 8 (2016) 17176–17186, https://doi.org/10.1021/acsami.6b05383.
[66] B. Zhang, H. Wang, S. Shen, X. She, W. Shi, J. Chen, Q. Zhang, Y. Hu, Z. Pang, X. Jiang, Fibrin-targeting peptide CREKA-conjugated multi-walled carbon nanotubes for self-amplified photothermal therapy of tumor, Biomaterials 79 (2016) 46–55, https://doi.org/10.1016/j.biomaterials.2015.11.061.
[67] X. Liang, W. Shang, C. Chi, C. Zeng, K. Wang, C. Fang, Q. Chen, H. Liu, Y. Fan, J. Tian, Dye-conjugated single-walled carbon nanotubes induce photothermal therapy under the guidance of near-infrared imaging, Canc. Lett. 383 (2016) 243–249, https://doi.org/10.1016/j.canlet.2016.09.006.
[68] Y. Hasin, M. Seldin, A. Lusis, Multi-omics approaches to disease, Genome Biol. 18 (2017) 83, https://doi.org/10.1186/s13059-017-1215-1.
[69] X. Peng, L. Pentassuglia, D.B. Sawyer, Emerging anticancer therapeutic targets and the cardiovascular system, Circ. Res. 106 (2010) 1022–1034, https://doi.org/10.1161/circresaha.109.211276.
[70] Y. Morita, M. Leslie, H. Kameyama, D. Volk, T. Tanaka, Aptamer therapeutics in cancer: current and future, Cancers 10 (2018) 80, https://doi.org/10.3390/cancers10030080.
[71] M. Gebauer, A. Skerra, Engineered protein scaffolds as next-generation therapeutics, Annu. Rev. Pharmacol. Toxicol. 60 (2020) 391–415, https://doi.org/10.1146/annurev-pharmtox-010818-021118.
[72] H.-Y. Cao, A.-H. Yuan, W. Chen, X.-S. Shi, Y. Miao, A DNA aptamer with high affinity and specificity for molecular recognition and targeting therapy of gastric cancer, BMC Canc. 14 (2014) 699, https://doi.org/10.1186/1471-2407-14-699.
[73] R. Bam, M. Laffey, K. Nottberg, P.S. Lown, B.J. Hackel, K.E. Wilson, Affibody-indocyanine green based contrast agent for photoacoustic and fluorescence molecular imaging of B7-H3 expression in breast cancer, Bioconjugate Chem. 30 (2019) 1677–1689, https://doi.org/10.1021/acs.bioconjchem.9b00239.
[74] R.R. Nani, A.P. Gorka, T. Nagaya, H. Kobayashi, M.J. Schnermann, Near-IR light-mediated cleavage of antibody-drug conjugates using cyanine photocages, Angew. Chem. Int. Ed. 54 (2015) 13635–13638, https://doi.org/10.1002/anie.201507391.
[75] R.R. Nani, A.P. Gorka, T. Nagaya, T. Yamamoto, J. Ivanic, H. Kobayashi, M.J. Schnermann, In vivo activation of duocarmycin-antibody conjugates by near-infrared light, ACS Cent. Sci. 3 (2017) 329–337, https://doi.org/10.1021/acscentsci.7b00026.
[76] A.P. Gorka, R.R. Nani, M.J. Schnermann, Harnessing cyanine reactivity for optical imaging and drug delivery, Acc. Chem. Res. 51 (2018) 3226–3235, https://doi.org/10.1021/acs.accounts.8b00384.
[77] T.A. Baudino, Targeted cancer therapy: the next generation of cancer treatment, Curr. Drug Discov. Technol. 12 (2015) 3–20, https://doi.org/10.2174/1570163812666150602144310.
[78] T. Yamaoka, S. Kusumoto, K. Ando, M. Ohba, T. Ohmori, Receptor tyrosine kinase-targeted cancer therapy, Int. J. Mol. Sci. 19 (2018) 3491, https://doi.org/10.3390/ijms19113491.
[79] S.M. Usama, B. Zhao, K. Burgess, A near-IR fluorescent dasatinib derivative that localizes in cancer cells, Bioconjugate Chem. 30 (2019) 1175–1181, https://doi.org/10.1021/acs.bioconjchem.9b00118.
[80] S.M. Usama, Z. Jiang, K. Pflug, R. Sitcheran, K. Burgess, Conjugation of dasatinib with MHI-148 has a significant advantageous effect in viability assays for glioblastoma cells, ChemMedChem 14 (2019) 1575–1579, https://doi.org/10.1002/cmdc.201900356.
[81] P.J. Choi, E. Cooper, P. Schweder, E. Mee, R. Faull, W.A. Denny, M. Dragunow, T.I. Park, J. Jose, The synthesis of a novel crizotinib heptamethine cyanine dye conjugate that potentiates the cytostatic and cytotoxic effects of Crizotinib in patient-derived glioblastoma cell lines, Bioorg. Med. Chem. Lett 29 (2019) 2617–2621, https://doi.org/10.1016/j.bmcl.2019.07.051.
[82] Q. Meng, Z. Liu, F. Li, J. Ma, H. Wang, Y. Huan, Z. Li, An HDAC-targeted imaging probe LBH589–Cy5.5 for tumor detection and therapy evaluation, Mol. Pharm. 12 (2015) 2469–2476, https://doi.org/10.1021/acs.molpharmaceut.5b00167.
[83] J.B. Wu, T.P. Lin, J.D. Gallagher, S. Kushal, L.W. Chung, H.E. Zhau, B.Z. Olenyuk, J.C. Shih, Monoamine oxidase A inhibitor-near-infrared dye conjugate reduces prostate tumor growth, J. Am. Chem. Soc. 137 (2015) 2366–2374, https://doi.org/10.1021/ja512613j.
[84] Q. Lv, D. Wang, Z. Yang, J. Yang, R. Zhang, X. Yang, M. Wang, Y. Wang, Repurposing antitubercular agent isoniazid for treatment of prostate cancer, Biomater. Sci. 7 (2019) 296–306, https://doi.org/10.1039/c8bm01189c.
[85] Y. Guan, Y. Zhang, L. Xiao, J. Li, J.P. Wang, M.D. Chordia, Z.Q. Liu, L.W. Chung, W. Yue, D. Pan, Improving therapeutic potential of farnesylthiosalicylic acid: tumor specific delivery via conjugation with heptamethine cyanine dye, Mol. Pharm. 14 (2017) 1–13, https://doi.org/10.1021/acs.molpharmaceut.5b00906.
[86] S. Hameed, P. Bhattarai, X. Liang, N. Zhang, Y. Xu, M. Chen, Z. Dai, Self-assembly of porphyrin-grafted lipid into nanoparticles encapsulating doxorubicin for synergistic chemo-photodynamic therapy and fluorescence imaging, Theranostics 8 (2018) 5501–5518, https://doi.org/10.7150/thno.27721.
[87] A.G. Arranja, V. Pathak, T. Lammers, Y. Shi, Tumor-targeted nanomedicines for cancer theranostics, Pharmacol. Res. 115 (2017) 87–95, https://doi.org/10.1016/j.phrs.2016.11.014.
[88] S. Hossen, M.K. Hossain, M.K. Basher, M.N.H. Mia, M.T. Rahman, M.J. Uddin, Smart nanocarrier-based drug delivery systems for cancer therapy and toxicity studies: a review, J. Adv. Res. 15 (2019) 1–18, https://doi.org/10.1016/j.jare.2018.06.005.
[89] C. Gao, P. Bhattarai, M. Chen, N. Zhang, S. Hameed, X. Yue, Z. Dai, Amphiphilic drug conjugates as nanomedicines for combined cancer therapy, Bioconjugate Chem. 29 (2018) 3967–3981, https://doi.org/10.1021/acs.bioconjchem.8b00692.
[90] F.U. Din, W. Aman, I. Ullah, O.S. Qureshi, O. Mustapha, S. Shafique, A. Zeb, Effective use of nanocarriers as drug delivery systems for the treatment of selected tumors, Int. J. Nanomed. 12 (2017) 7291–7309, https://doi.org/10.2147/ijn.s146315.
[91] Y.I. Chen, C.L. Peng, P.C. Lee, M.H. Tsai, C.Y. Lin, Y.H. Shih, M.F. Wei, T.Y. Luo, M.J. Shieh, Traceable self-assembly of laser-triggered cyanine-based micelle for synergistic therapeutic effect, Adv. Healthcare Mater. 4 (2015) 892–902, https://doi.org/10.1002/adhm.201400729.
[92] I. Noh, M. Kim, J. Kim, D. Lee, D. Oh, J. Kim, C. Kim, S. Jon, Y.C. Kim, Structure-inherent near-infrared bilayer nanovesicles for use as photoacoustic image-guided chemo-thermotherapy, J. Contr. Release 320 (2020) 283–292, https://doi.org/10.1016/j.jconrel.2020.01.032.
[93] C. Jeong, I. Noh, N.S. Rejinold, J. Kim, S. Jon, Y.-C. Kim, Self-assembled supramolecular bilayer nanoparticles composed of near-infrared dye as a theranostic nanoplatform to encapsulate hydrophilic drugs effectively, ACS Biomater. Sci. Eng. 6 (2019) 474–484, https://doi.org/10.1021/acsbiomaterials.9b01587.
[94] E. De Los Reyes-Berbel, R. Salto-Gonzalez, M. Ortega-Munoz, F.J. Reche-Perez, A.B. Jodar-Reyes, F. Hernandez-Mateo, M.D. Giron-Gonzalez, F. Santoyo-Gonzalez, PEI-NIR heptamethine cyanine nanotheranostics for tumor targeted gene delivery, Bioconjugate Chem. 29 (2018) 2561–2575, https://doi.org/10.1021/acs.bioconjchem.8b00262.
[95] S. Hua, M.B.C. de Matos, J.M. Metselaar, G. Storm, Current trends and challenges in the clinical translation of nanoparticulate nanomedicines: pathways for translational development and commercialization, Front. Pharmacol. 9 (2018) 790, https://doi.org/10.3389/fphar.2018.00790.